MOLECULAR AND CELLULAR BIOLOGY, May 2004, p. 4275–4293 Vol. 24, No. 10
0270-7306/04/$08.00+0 DOI: 10.1128/MCB.24.10.4275–4293.2004

Constitutive Expression of Tert in Thymocytes Leads to Increased Incidence and Dissemination of T-Cell Lymphoma in Lck-Tert Mice

Andrés Canela,[1] Juan Martín-Caballero,[2] Juana M. Flores,[3] and María A. Blasco[1]*

Telomeres and Telomerase Group, Molecular Oncology Program,[1] and Biotechnology Program,[2] Spanish National Cancer Centre (CNIO), 28029 Madrid and Department of Animal Pathology II, Universidad Complutense de Madrid, 28040 Madrid,[3] Spain

Received 20 October 2003/Returned for modification 23 November 2003/Accepted 20 January 2004

Here we describe a new mouse model with constitutive expression of the catalytic subunit of telomerase (Tert) targeted to thymocytes and peripheral T cells (Lck-Tert mice). Two independent Lck-Tert mouse lines showed higher incidences of spontaneous T-cell lymphoma than the corresponding age-matched wild-type controls, indicating that constitutive expression of Tert promotes lymphoma. Interestingly, T-cell lymphomas in Lck-Tert mice were more disseminated than those in wild-type controls and affected both lymphoid and nonlymphoid tissues, while nonlymphoid tissues were never affected with lymphoma in age-matched wild-type controls. Importantly, these roles of Tert constitutive expression in promoting tumor progression and dissemination were independent of the role of telomerase in telomere length maintenance, since telomere length distributions on a single-cell basis were identical in Lck-Tert and wild-type thymocytes. Finally, Tert constitutive expression did not interfere with telomere capping in Lck-Tert primary thymocytes, although it resulted in greater chromosomal instability upon gamma irradiation in Lck-Tert primary lymphocytes than in controls, suggesting that Tert overexpression may interfere with the cellular response to DNA damage.

Telomerase activity can provide limitless proliferative capacity, a hallmark of human cancer, through its ability to elongate telomeres (2). The majority of human tumors activate telomerase at some point during their development (27). The role of telomerase in tumor cells has been assumed to be restricted to preventing TTAGGG exhaustion from chromosome ends, which otherwise would trigger cell arrest and/or apoptosis (2). More recently, however, forced telomerase expression in cells and mice with sufficiently long telomeres has shown that telomerase can also promote growth and survival in a manner which appears to be uncoupled from net telomere lengthening (5). Mounting evidence for this novel role of telomerase in tumorigenesis has been obtained from studying mouse models. Telomerase activity is upregulated during mouse tumorigenesis, despite the fact that mice have very long telomeres (3, 9). In addition, mice that overexpress the catalytic component of mouse telomerase under the control of a keratin 5 promoter (K5-Tert mice) are more susceptible to developing both carcinogen-induced and spontaneous tumors (14, 16). Mice with transgenic telomerase expression under the control of a β-actin constitutive promoter also have an increased incidence of spontaneous tumors as they age (1). These findings suggest that constitutive transgenic telomerase expression promotes tumorigenesis in mice with very long telomeres. However, the mechanisms by which constitutive expression of the catalytic subunit of telomerase (Tert) promotes tumorigenesis independently of telomere length remain unknown.

Here we describe the generation of a new mouse model with Tert constitutive expression specifically targeted to the thymus by use of the Lck promoter (Lck-Tert mice). We show here that these mice are prone to developing spontaneous T-cell lymphoma, thus providing further evidence that telomerase promotes tumorigenesis independently of telomere length when it is constitutively expressed in thymocytes. Strikingly, spontaneous T-cell lymphomas present in Lck-Tert mice were more disseminated than those in wild-type controls: they affected a higher number of lymphoid tissues, as well as nonlymphoid organs, which were never affected in age-matched wild-type controls. These findings indicate that constitutive Tert expression targeted to T cells not only promotes T-cell lymphomas in Lck-Tert mice but also makes these T-cell lymphomas more invasive than those of wild-type mice, thus unveiling a novel role of telomerase in sustaining tumor dissemination.

Finally, the construction of Lck-Tert mice allowed us to study whether Tert overexpression interfered with proper telomere capping by using quantitative fluorescence in situ hybridization (Q-FISH) on metaphase spreads from wild-type and Lck-Tert primary thymocytes. Telomere function was intact in Lck-Tert thymocytes, indicating that overexpressed Tert does not interfere with the formation of a proper telomere capping structure. However, Tert constitutive expression resulted in greater chromosomal instability upon gamma irradiation in Lck-Tert primary lymphocytes than in wild-type littermate controls, suggesting an impact of Tert overexpression on the DNA damage response and pinpointing new ways by which Tert may promote tumorigenesis.

* Corresponding author. Mailing address: Spanish National Cancer Centre (CNIO), Melchor Fernandez Almagro 3, E-38029 Madrid, Spain. Phone: 34 917328031. Fax: 34 917328028. E-mail: mblasco@cnio.es.

MATERIALS AND METHODS

Generation of Lck-Tert transgenic mice. An EcoRI fragment containing the full-length mouse Tert cDNA and 3′ untranslated sequences (23) was cloned into a vector harboring the proximal Lck promoter as well as partial sequences of the

human growth hormone (hGH) gene, which were introduced to confer stability on the mRNA (10); the resulting construct was named Lck-Tert (see Fig. 1A). It is noteworthy that the final Lck-Tert construct contained the full-length mTert cDNA including its own stop codon, as well as 3′ untranslated sequences (Fig. 1A). Therefore, Tert is not expressed as a fusion protein with hGH sequences, and the phenotypes shown here for Lck-Tert mice are not likely to result from the presence of partial hGH gene sequences in the targeting construct. This is also supported by the fact that many transgenic mice have been generated in recent years by using this type of targeting vector, and they have shown phenotypes that were attributable to the particular gene expressed and not to the partial hGH sequences (see, for example, reference 20). A linear NotI restriction fragment containing the Lck-Tert transgene was injected into the pronuclei of fertilized oocytes from C57BL/6 × CBA F_1 mice (Fig. 1A). Microinjected eggs were transferred to recipient pseudopregnant females at the 2-cell stage. Genotyping was performed by PCR as described below. Transgenic founder mice were backcrossed for four to six generations onto a C57BL/6 background to produce the different mouse lines. The wild-type and Lck-Tert mice used from each transgenic line were always littermates and therefore had identical genetic backgrounds.

Mouse genotyping. Transgenic Lck-Tert mice were genotyped by PCR using a set of primers directed against hGH sequences in the targeting vector (20): hGH-3′ (5′-GCACACGCTGAGCTAGGTTCCC-3′) and hGH-4′ (5′ CATAG ACGTTGCTGTCAGAGGC-3′). The size of the expected amplified product was 415 bp. As an internal control for PCR efficiency, we used primers directed against the thyroid-stimulating hormone β (TSHβ) gene: TSHβ-5′ (5′-TCCTC AAAGATGCTCATTAG-3′) and TSHβ-3′ (5′-GTAACTCACTCATGCA-3′). In this case, the expected size of the amplified fragment was 386 bp.

Mouse breeding and housing. Large colonies of the different Lck-Tert mouse lines were obtained and maintained at the National Center for Biotechnology under specific-pathogen-free conditions in accordance with the recommendations of the Federation of European Laboratory Animal Science Associations.

Histology and immunohistochemistry. Histopathology was performed on 2-year-old wild-type and Lck-Tert mice as described previously (25).

For immunohistochemistry, tissue sections were processed with 10 mM citrate buffer (pH 6.0) in a microwave (at 100°C for 15 min), and endogenous peroxidase activity was inactivated by incubation with 3% hydrogen peroxide in methanol (for 15 min at room temperature). Sections were then incubated in a humidity chamber with either (i) a rat anti-mouse CD45R/B220 monoclonal antibody for B-lymphocyte detection (dilution, 1:100; overnight incubation at 4°C; Southern Biotechnology Associates, Birmingham, Ala.), (ii) a rabbit anti-human CD3 polyclonal antibody for T-lymphocyte detection (dilution, 1:100; overnight incubation at 4°C; DakoCytomation, Glostrup, Denmark), (iii) a rabbit anti-TdT polyclonal antibody for terminal deoxynucleotidyl transferase detection (dilution, 1:10; 40-min incubation at room temperature; Supertechs, Bethesda, Md.), or (iv) a rabbit anti-immunoglobulin M (IgM) polyclonal antibody for IgM detection (dilution, 1:400; 40-min incubation at room temperature; DakoCytomation). The antibodies were diluted in Tris-buffered saline (TBS). After three 5-min washes in TBS, samples were incubated with a secondary antibody. For detection of the primary rabbit polyclonal antibody against human CD3, we used biotinylated goat anti-rabbit IgG (dilution, 1:400; Vector Laboratories, Burlingame, Calif.), and for the other primary rabbit antibodies, we used a horseradish peroxidase-conjugated goat anti-rabbit antibody (DakoCytomation). For primary rat antibodies, biotinylated rabbit anti-rat IgG was used (Vector). In the case of biotinylated secondary antibodies, after 30 min with the secondary antibody, sections were incubated for 30 min at room temperature with peroxidase-conjugated streptavidin diluted 1:20 in TBS (Zymed Laboratories, Inc.). The chromogen was 3-3′-diaminobenzidine tetrahydrochloride (Sigma), diluted 0.002% in TBS in the presence of 0.01% hydrogen peroxide. Nuclei were counterstained with Harris hematoxylin for 1 min. Primary antibodies were replaced with TBS and rat and rabbit nonimmune serum in negative controls. Normal lymphoid tissue was used as a positive control.

Telomerase assay. S-100 extracts were prepared from the indicated tissues, and a telomerase repeat amplification protocol (TRAP) assay was used to measure telomerase activity (3). An internal control for PCR efficiency was included (TRAPeze kit; Oncor). TRAP products were quantified by using either a Storm PhosphorImager and ImageQuant, version 1.2 (both from Molecular Dynamics) or NIH Image (version 1.62) software.

Telomere length determination. (i) Q-FISH. Freshly isolated thymocytes and lymph node cells from 6-week-old wild-type and Lck-Tert littermates, as well as cells derived from lymphomas, were prepared, and Q-FISH was performed as described previously (12). Images were captured by using Leica Q-FISH software as described previously (12). TFL-Telo software (a gift from P. Lansdorp, Vancouver, Canada) was used to quantify the fluorescence intensities of telomeres from 7 to 10 metaphases of each data point. Telomeres below the Q-FISH detection limit (150 to 300 bp) were considered undetectable, or "signal-free ends." Images of metaphases from littermates were captured on the same day and scored in a blinded fashion.

(ii) Flow-FISH. Freshly isolated cells from the indicated lymphoid tissues of 24-month-old mice were prepared as described in reference 7, and flow cytometry-FISH (flow-FISH) was performed as described previously (12). Telomere fluorescence of at least 2,000 cells gated at the G_1/G_0 cell cycle stage was measured by using a Coulter flow EPICS XL cytometer with SYSTEM 2 software.

(iii) TRF analysis. Freshly isolated cells from lymphoid tissues of 24-month-old mice were prepared as described in reference 7, and telomere restriction fragment (TRF) analysis was performed as described by Blasco et al. (7).

Real-time quantitative RT-PCR for detection of Tert mRNA in Lck-Tert and wild-type mice. Two to three age-matched (3-month-old) wild-type and Lck-Tert mice from each mouse line were sacrificed in parallel, and total RNA was extracted with Trizol from the indicated organs and tissues (Life Technologies, Inc., Rockville, Md.). The same procedures were followed to analyze Tert mRNA expression in fluorescence-activated cell sorter (FACS)-sorted cell subsets (5-week-old mice) and in tumoral and nontumoral organs (2-year-old mice). Reverse transcription (RT) was performed by using 5 μg of total RNA, random hexamers, and Superscript II reverse transcriptase (Life Technologies) according to the manufacturer's instructions. Real-time PCR was performed with a LightCycler instrument (Roche, Mannheim, Germany) or with an ABI PRISM 7700 instrument (Applied Biosystems, Foster City, Calif.), by using either FastStart DNA Master SYBR Green I mix (Roche) or SYBR Green PCR Core Reagents (Applied Biosystems), respectively. The final $MgCl_2$ concentration was 4.5 μM, and primers were used at 0.4 μM. Reaction mixtures were incubated either for 5 min at 95°C followed by 40 PCR cycles in the LightCycler (15 s at 95°C, 25 s at 68°C, and 5 s at 80°C) or for 10 min at 95°C followed by 40 PCR cycles in the ABI PRISM 7700 (15 s at 95°C, 90 s at 67°C). Relative Tert expression was determined by using β-actin mRNA-normalized standard curves or by calculating $\Delta\Delta C_t$ values, which express the difference between the cycle threshold of the Tert primer pair and that of the β-actin mRNA primer pair. Primers used were TERT-F (5′ GGA TTG CCA CTG GCT TCC G 3′) and TERT-R (5′ TGC CTG ACC TCC TCT TGT GAC 3′), referred to below as A primers. Parallel RT-PCRs were carried out for actin by using primers ACTIN-F (5′ GGC ACC ACA CCT TCT ACA ATG 3′) and ACTIN-R (5′ GTG GTG GTG AAG CTG TAG 3′). In all cases, each PCR was repeated at least twice.

Real-time quantitative RT-PCR for detection of Lck-Tert mRNA in Lck-Tert mice. Total RNA was extracted from Lck-Tert mice (tissues, cells, and tumors), and RT and real-time PCR were performed as described above. The expected size of the Lck-Tert-specific band was 160 bp. The transgene-specific hGHp2 primers contain exon-3 sequences at the 3′ end and exon-2 or exon-4 sequences at the 5′ end in the forward or reverse primer, respectively (hGHp2F [5′ TGA CAC CTA CCA GGA GTT TGA AGA 3′] and hGHp2R [5′ GAT GCG GAG CAG CTC TAG GTT GGA 3′]). Parallel RT-PCRs were carried out for actin as described above. In all cases, each PCR was repeated at least twice. For each mRNA, Lck-Tert expression was determined by using β-actin mRNA-normalized standard curves or by calculating $\Delta\Delta C_t$ values, which express the cycle threshold difference between the Lck-Tert primer pair and the β-actin mRNA primer pair.

Sorting of lymphoid populations from the spleen, thymus, and lymph nodes. Single-cell suspensions from the thymus, spleen, and lymph nodes were prepared from age-matched (5-week-old) wild-type and Lck-Tert mice by mincing samples through a 10-μm-pore-size nylon mesh. For cell surface staining before FACS, antibodies were conjugated to fluorescein isothiocyanate (FITC), phycoerythrin (PE), or Spectral Red (SPRD). Antibodies against CD8a (Lyt-2, -53, and -6.7) (Southern Biotechnology) and against CD4 (L3T4, RM4-5), CD3e, and B220 (CD45R, RA3-6B2) (PharMingen, San Diego, Calif.) were used. Sorting was performed with a FACS (FACSort flow cytometer; Becton Dickinson, Mountain View, Calif.). The sorted cell populations were >99.5% pure on reanalysis (data not shown).

(i) Thymocyte subsets. Thymocytes were sorted after staining with PE-conjugated anti-CD4 and SPRD-conjugated anti-CD8. The following populations were obtained: double-negative cells ($CD4^-$ $CD8^-$), double-positive cells ($CD4^+$ $CD8^+$), CD4 single-positive cells ($CD4^+$ $CD8^-$), and CD8 single-positive cells ($CD4^-$ $CD8^+$).

(ii) Spleen and lymph node subsets. The following cell populations were sorted from spleens and lymph nodes after triple staining with FITC-conjugated anti-CD3, PE-conjugated anti-CD4, and SPRD-conjugated anti-CD8: $CD4^+$ T cells ($CD3^+$ $CD4^+$) and $CD8^+$ T cells ($CD3^+$ $CD8^+$). In the case of the spleen only, the following populations were sorted after double staining with FITC-

conjugated anti-CD3 and PE-conjugated anti-B220: B cells ($B220^+$) and "non-B, non-T cells" ($B220^-$ $CD3^-$).

Hematology analyses. Peripheral blood was extracted from 22- to 27-week-old mice and was analyzed by using a Procount hematology analyzer (ABX Diagnostics, Montpellier, France). The reference range for each cell type was 4×10^9 to 12×10^9 cells/liter for white blood cells ($<4 \times 10^9$ cells/liter, leukopenia; $>12 \times 10^9$ cells/liter, leukocytosis), 2×10^9 to 9×10^9 cells/liter for lymphocytes ($<2 \times 10^9$ cells/liter, lymphopenia; $>9 \times 10^9$ cells/liter, lymphocytosis), 0.70×10^9 to 6×10^9 cells/liter for granulocytes ($<0.70 \times 10^9$ cells/liter, granulopenia; $>6 \times 10^9$ cells/liter, granulocytosis). Normal reference values for the "blood formula" were 50 to 75% lymphocytes and 10 to 25% granulocytes (we considered the blood formula to be "altered" when the ratio of lymphocytes to granulocytes was inverted). Finally, normal reference counts for red blood cells were 9×10^{12} to 15×10^{12} cells/liter ($<9 \times 10^{12}$ cells/liter, anemia; $>15 \times 10^{12}$ cells/liter, polycytemia) and a hematocrit of 27 to 45%.

FACS analysis of lymphomas. To characterize the immunophenotype of spontaneous lymphomas appearing in Lck-Tert and wild-type mice, single-cell suspensions were prepared from the affected organs and stained with antibodies specific for mouse T and B cells. Antibodies were FITC-conjugated anti-CD4 (L3T4) and anti-CD8a (Ly-2), PE-conjugated anti-CD4 (L3T4) and anti-CD8a (Ly-2), Tricolor-conjugated anti-CD3e, and allophycocyanin-conjugated anti-B220 (CD45R) and anti-CD3e (all antibodies were from PharMingen). A FACScalibur cytometer (Becton Dickinson) equipped with Cellquest Pro software (Becton Dickinson), which has the capacity to analyze four different fluorochromes simultaneously, was used for the analysis.

PCR analysis of lymphoma clonality. Genomic DNA was isolated from organs affected with lymphoma by standard procedures. T-cell receptor β (TCRβ) gene clonality was assayed at V-DJ and D-J rearrangements by four different PCRs using the primers and conditions described previously (13). In particular, for TCRβ, a mixture of 20 family-specific upstream primers within Vβ gene segments (designated Vβ primers here [Fig. 6D through G] and Vn-S primers in reference 13), consensus primers located immediately 5′ of Dβ1 and Dβ2 gene segments (designated primers Dβ1 and Dβ2 here [Fig. 6D through G] and primers D1U-S and D2U-S, respectively, in reference 13), and consensus downstream primers immediately 3′ of Jβ1 and Jβ2 gene segments (designated primers Jβ1 and Jβ2 here [Fig. 6D through G] and primers J1D-A and J2D-A, respectively, in reference 13) were used. TCRγ gene clonality was assayed at V-J rearrangements by using consensus primers Vγ4 and Jγ1 as described previously (21). IgH gene clonality was assayed at D-J rearrangements with consensus primers DSF and JH4 as described previously (21). PCR primers Jβ1, Jβ2, Jγ1, and JH4 were labeled at the 5′ end with 6-carboxyfluorescein (6-Fam) to allow gene scanning of the PCR products. Each PCR was performed at least twice. Fluorochrome-labeled, single-stranded (denatured) PCR products were analyzed by capillary electrophoresis using the ABI PRISM 3700 Genetic Analyzer and GeneScan software (Applied Biosystems, Weiterstadt, Germany) according to the manufacturer's procedures.

Gamma irradiation and karyotypic analysis. Single-dose whole-body gamma irradiation (4 Gy) of age-matched (6-week old) wild-type and Lck-Tert mice from lines M17 and M40 was performed by using a ^{137}Cs source (MARK 1-30 irradiator; Shepherd & Associates) at a rate of 2.11 Gy/min. Immediately upon irradiation, mice were sacrificed, and fresh thymocytes were isolated as described previously (25). In parallel, thymocytes were isolated from nonirradiated, age-matched (6-week-old) wild-type and Lck-Tert mice of lines M17 and M40, used as controls. In all cases, fresh thymocytes were stimulated with phorbol myristate acetate (50 ng/ml) and ionomycin (500 ng/ml) (Calbiochem, San Diego, Calif.) to proliferate in culture. Seventy-two hours after mitogen addition, cells were prepared for telomere Q-FISH as described previously (12), which allows determination of the involvement of telomeres in chromosomal aberrations. Fifty to 100 metaphases were scored for chromosomal aberrations in each thymocyte culture. Aberrations were classified into end-to-end fusions (Robertsonian-like fusions [RLF], rings, and various types of dicentric and tricentric chromosomes), fragments (fragment arms, centric chromosomes, acentric chromosomes, and fragment blots), and telomeric associations (TA). TA was scored when two chromosomes were close but not fusionated and the telomeric signals were aligned and equidistant from the end of one chromosome to the other and separated by less than half of the chromatid thickness. The percentage of metaphases that did not show any chromosomal aberration is also indicated.

Proliferation assays with wild-type and Lck-Tert primary thymocytes. For evaluation of proliferation, [^{3}H]thymidine incorporation assays were performed. A total of 25,000, 75,000, 150,000, and 300,000 primary thymocytes from each genotype were plated in triplicate in 96-well microtiter plates and stimulated to proliferate in culture by use of phorbol myristate acetate (50 ng/ml) and ionomycin (500 ng/ml) (Calbiochem) in the presence of 0.1, 1, or 10% fetal bovine serum (Cambrex). Forty-eight hours after the cultures were started, DNA synthesis was measured by incubating cells in 5 μCi of [*methyl*-^{3}H]thymidine (2 Ci/mmol; Amersham)/ml. After 18 h of incubation, the incorporation of radioactivity into DNA was measured by using an LKB 1295-001 cell harvester and a Betaplate 1205 scintillation counter.

Measurement of apoptosis in wild-type and Lck-Tert primary thymocytes. Primary thymocytes were cultured at a density of 10^6/ml in a medium with 10, 1, 0.1, or 0% fetal bovine serum (Cambrex). After 24 and 48 h, cell death was measured by propidium iodide staining (DNA-Prep; Coulter) and cell cytometry (Epics XL cytometer; Coulter Corporation). Cells in G_0/G_1, S, and G_2/M were considered to be surviving cells.

Statistical calculations. A two-tailed Student *t* test with "two-sample unequal variance" was used to assess the statistical significance of lymphoma incidence, as well as that of the numbers of organs affected with lymphoma. GraphPad Prism (version 3.0a) and Microsoft Excel (version 2001) were used for statistical calculations. To evaluate the severity of lymphomas, we arbitrarily defined a "lymphoma severity index" as follows: 0, mouse with no lymphoma; 1, mouse with lymphoma affecting only one lymphoid organ; 2, mouse with lymphoma affecting more than one lymphoid organ; 4, mouse with lymphoma affecting nonlymphoid tissues.

RESULTS

Targeted expression of Tert to the thymus: Lck-Tert mice. We generated Lck-Tert mice, transgenic mice that express the murine Tert cDNA under the control of the p56lck proximal promoter (see Materials and Methods), which targets Tert overexpression to thymocytes and peripheral T cells (Fig. 1A). A total of four independent Lck-Tert transgenic lines (M15, M17, M40, and M41) were obtained. (For mouse generation, genotyping, and mouse housing, see Materials and Methods.)

To determine Tert mRNA levels in thymocytes from both transgenic and wild-type littermates, we performed real time RT-PCR using primers directed against the mouse Tert coding sequence (Fig. 1A, A primers) (see Materials and Methods). These primers amplify both endogenous and transgenic Tert mRNA. Lck-Tert mice of the M15 line showed Tert mRNA levels that were only slightly (1.5 ± 0.9-fold) increased over those for wild-type controls (not statistically significant), suggesting that the transgene is not expressed in this Lck-Tert line (Fig. 1B). The absence of transgenic Tert expression in the M15 line could be due to the insertion of the transgene in the Y chromosome (with a high heterochromatin content), as suggested by the fact that only males carried the transgene (data not shown). In contrast, Lck-Tert mice of the M17, M40, and M41 lines showed 129- to 789-fold more Tert mRNA in the thymus than their wild-type littermates (Fig. 1B), indicating that the transgene was being vastly overexpressed (see below).

To study the whole-body expression pattern of the Lck-Tert transgene, Tert mRNA levels were determined in a variety of tissues from Lck-Tert mice and wild-type littermates. Figure 1C shows Tert mRNA levels for the M40 line. Tert overexpression was largely specific to the thymus, although it was also found in other lymphoid tissues from Lck-Tert mice, such as the spleen (7-fold increase in Tert expression over that for wild-type mice) and lymph nodes (40-fold increase), as well as in the brain (16-fold increase) (Fig. 1C). The rest of the Lck-Tert tissues analyzed showed no or very low increases in Tert mRNA levels over those in the controls (Fig. 1C). To demonstrate that the transgenic Lck-Tert mRNA was expressed in these different tissues, we performed real-time RT-PCR using primers specific for the transgenic Lck-Tert mRNA that do not amplify the endogenous Tert mRNA in Lck-Tert mice

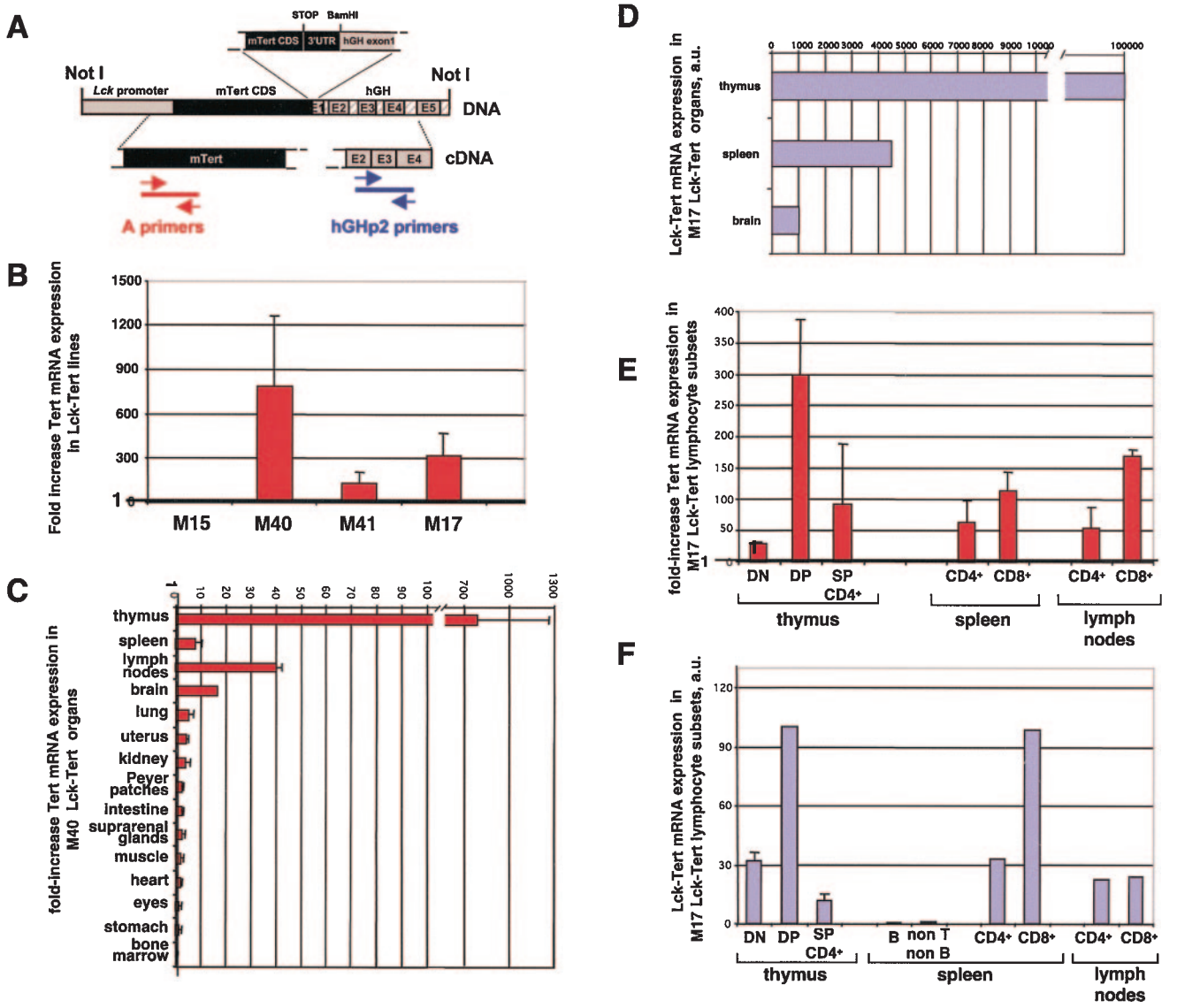

FIG. 1. (A) Lck-Tert DNA construct used for transgenesis. mTert, mouse Tert; CDS, coding sequence; STOP, mTert stop codon; 3′ UTR, 3′ untranslated sequences. Primers used for real-time quantitative RT-PCR detection of both endogenous and Lck-Tert mRNA (A primers, in red) or for detection of Lck-Tert mRNA only (hGHp2 primers, in blue) are indicated. (B) Ratio of Tert mRNA abundance in Lck-Tert thymuses to that in wild-type thymuses from several independent transgenic lines (M15, M40, M41, and M17) as determined by real time RT-PCR using A primers. (C) Ratio of Tert mRNA abundance in M40 Lck-Tert organs to that for wild-type littermates as determined by real time RT-PCR using A primers. (D) Transgenic Lck-Tert mRNA abundance (expressed in arbitrary units [a.u.]) in the indicated M17 Lck-Tert tissues, determined by using hGHp2 primers. (E) Ratio of Tert mRNA abundance in isolated lymphoid populations from the indicated lymphoid tissues of Lck-Tert mice to that for wild-type littermates as determined by real time RT-PCR using A primers. DN, double-negative cells ($CD4^-$ $CD8^-$); DP, double-positive cells ($CD4^+$ $CD8^+$); SP, single-positive cells. (F) Abundance of transgenic Lck-Tert-specific mRNA in isolated lymphoid cells from Lck-Tert mice as determined by real time RT-PCR using hGHp2 primers. Lck-Tert levels in total cells from the thymus were assigned the value of 100 a.u., and Lck-Tert levels in isolated populations were expressed relative to that value. B, cells positive for the B220 marker; non-B, non-T, cells that did not stain for the B220 marker or the CD3 marker (specific for T cells).

(hGHp2 primers) (see Fig. 1A and Materials and Methods). Transgenic Lck-Tert mRNA was abundantly expressed in the thymuses, spleens, and brains of M17 Lck-Tert mice, showing 100,000, 45,100, and 1,000 arbitrary units of expression, respectively (Fig. 1D), but was undetectable in wild-type littermates of the same line (data not shown). We next determined Tert mRNA levels in isolated T- and B-cell populations from the different lymphoid organs of Lck-Tert mice (see Materials and Methods). As shown for the M17 line in Fig. 1E, Tert mRNA levels were increased in all T-cell populations of the Lck-Tert thymus compared to the wild-type thymus, and double-positive T cells ($CD4^+$ $CD8^+$) showed the highest overexpression of Tert mRNA levels. In the case of the spleen and lymph nodes, Tert mRNA levels were increased in T cells (both $CD4^+$ and $CD8^+$) compared to wild-type controls (Fig. 1E) (see Materials and Methods). In addition, we performed real-time RT-

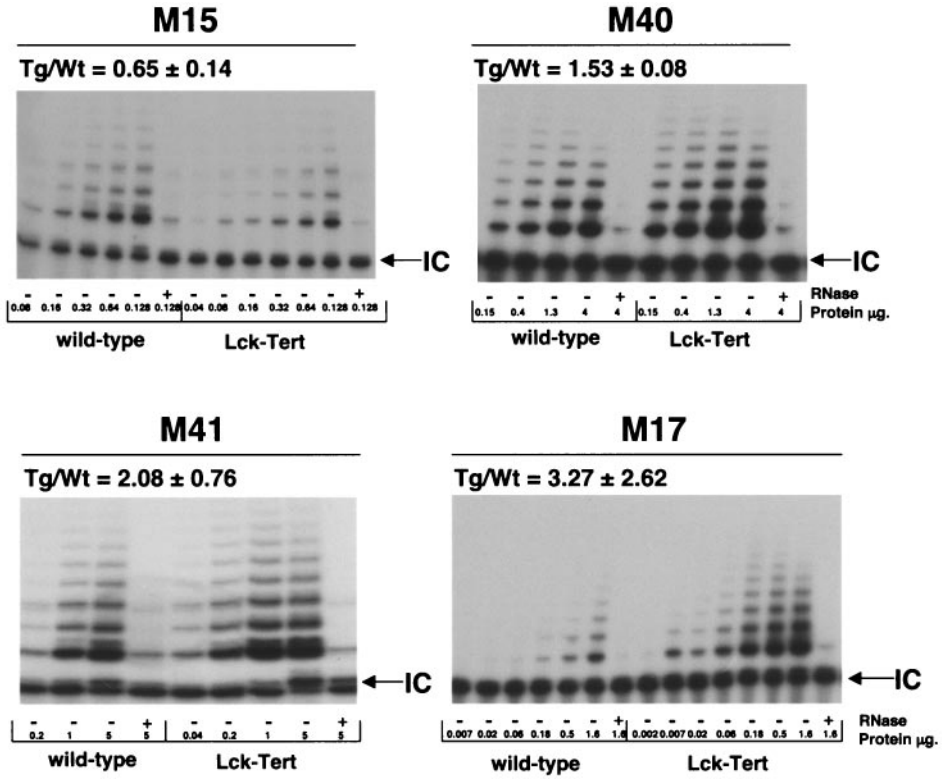

FIG. 2. Telomerase activity as detected by the TRAP assay in the thymuses of wild-type and Lck-Tert littermates of the indicated mouse lines. The S-100 extract concentrations assayed are indicated. − or +, extracts not treated or treated with RNase, respectively. IC, internal control for PCR efficiency. The ratio of the average TRAP activity in the thymuses of transgenic (Tg) Lck-Tert mice to that for wild-type (Wt) mice (from at least two mice of each genotype), together with the standard deviation, is shown for each mouse line.

PCR using hGHp2 primers. Transgenic Lck-Tert mRNA was abundantly expressed in the different T-cell populations of the thymus, with the highest abundance in double-positive T cells, as well as in the T-cell populations of the spleen and lymph nodes (both $CD4^+$ and $CD8^+$) (Fig. 1F). Importantly, B cells (positive for the B220 marker) and immune cells that did not stain with B- or T-cell markers (non-B, non-T cells) showed only background levels of Lck-Tert mRNA expression (Fig. 1F). These results indicate that transgenic Lck-Tert expression is specifically targeted to thymocytes and peripheral T cells, in agreement with the known expression pattern of the p56lck proximal promoter (30).

Increased telomerase activity in Lck-Tert thymocytes compared to control wild-type thymocytes. We measured telomerase activity in thymuses from at least two pairs of Lck-Tert and wild-type littermates for each of the different transgenic lines by using the TRAP assay (Fig. 2) (see Materials and Methods). Mice of line M15, with null transgenic Lck-Tert mRNA expression, did not show higher TRAP activity in the thymus than wild-type littermates (Fig. 2). TRAP activity was increased in the thymuses of M40, M41, and M17 Lck-Tert mice compared to that in their wild-type littermates from the same lines, as indicated by increases in the intensities of the TRAP products (Fig. 2) (see Materials and Methods). TRAP assays were performed under linear conditions of product amplification, which allowed for quantification of TRAP activity levels. The Lck-Tert/wild-type TRAP signal ratios were 0.65 ± 0.14, 1.53 ± 0.08, 2.08 ± 0.76, and 3.27 ± 2.62 for the M15, M40, M41, and M17 lines, respectively (see Materials and Methods).

The fact that TRAP activity is approximately twofold higher in Lck-Tert thymuses than in wild-type controls is surprising given the fold overexpression of Tert mRNA in transgenic thymuses, described above (Fig. 1B). This fact could be explained if one considers that wild-type thymocytes already contain active telomerase, and it is likely that the vast overexpression of Tert in transgenic cells is saturating the formation of active telomerase complexes with the telomerase RNA component (Terc), which may be rate-limiting under these conditions.

Similar telomere length distributions in wild-type and Lck-Tert lymphoid tissues. We measured telomere lengths in thymocytes and peripheral T cells derived from age-matched (6 week-old) Lck-Tert mice and wild-type littermates. For this purpose, we determined telomere fluorescence after hybridization with a peptide nucleic acid-telomeric probe by using Q-FISH and flow-FISH (see Materials and Methods). Q-FISH measures the lengths of all individual telomeres on metaphase spreads and allows distributions of telomere length frequencies to be obtained (Fig. 3A). Measurement of the telomere length of each individual chromosome is essential, because telomerase overexpression may alter the normal telomere length distribution in Lck-Tert cells from that in wild-type controls. In particular, short telomeres are more likely to be deregulated as

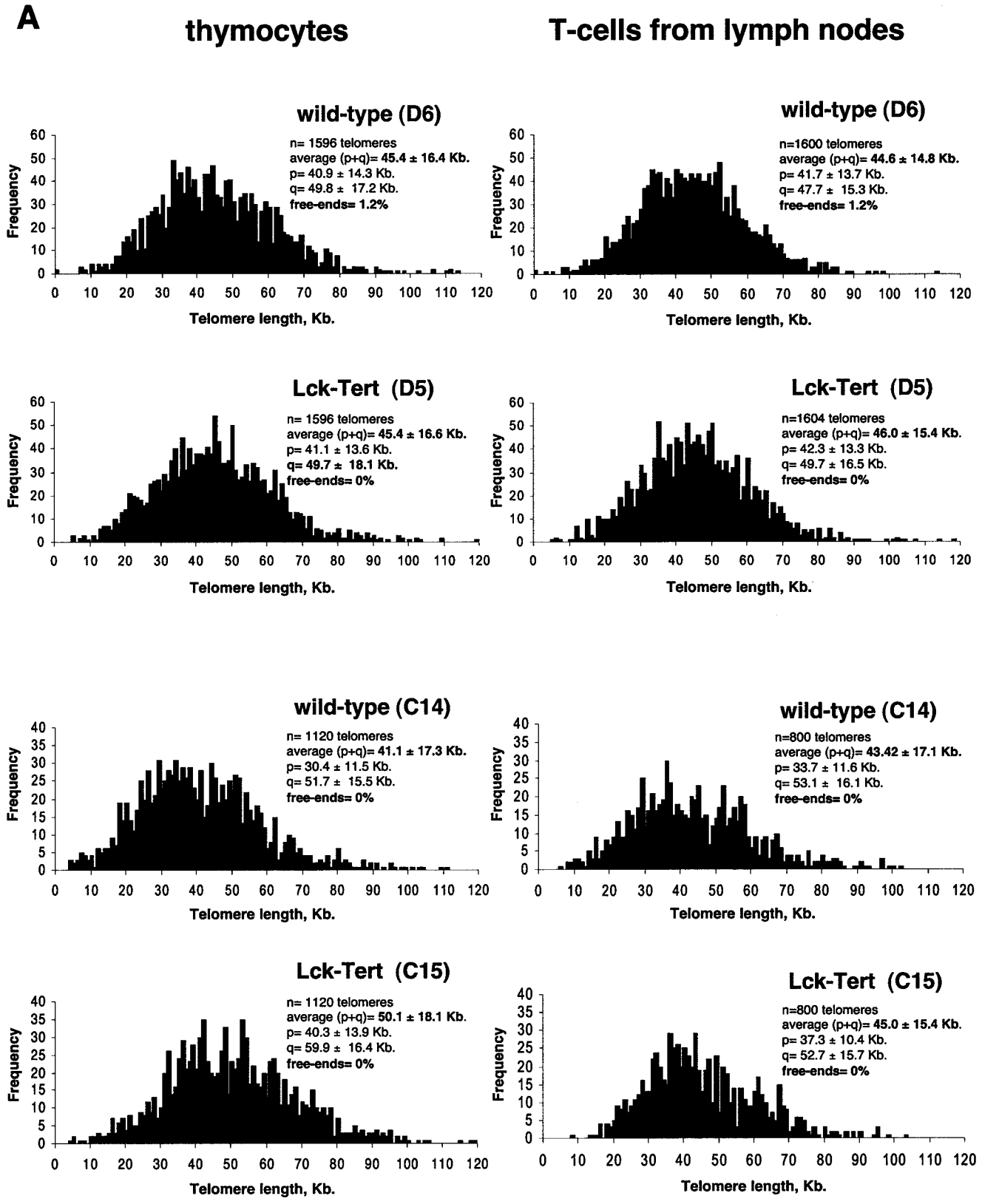
A
thymocytes
T-cells from lymph nodes
wild-type (D6)
n= 1596 telomeres
average (p+q)= 45.4 ± 16.4 Kb.
p= 40.9 ± 14.3 Kb.
q= 49.8 ± 17.2 Kb.
free-ends= 1.2%
wild-type (D6)
n=1600 telomeres
average (p+q)= 44.6 ± 14.8 Kb.
p= 41.7 ± 13.7 Kb.
q= 47.7 ± 15.3 Kb.
free-ends= 1.2%
Lck-Tert (D5)
n= 1596 telomeres
average (p+q)= 45.4 ± 16.6 Kb.
p= 41.1 ± 13.6 Kb.
q= 49.7 ± 18.1 Kb.
free-ends= 0%
Lck-Tert (D5)
n=1604 telomeres
average (p+q)= 46.0 ± 15.4 Kb.
p= 42.3 ± 13.3 Kb.
q= 49.7 ± 16.5 Kb.
free-ends= 0%
wild-type (C14)
n= 1120 telomeres
average (p+q)= 41.1 ± 17.3 Kb.
p= 30.4 ± 11.5 Kb.
q= 51.7 ± 15.5 Kb.
free-ends= 0%
wild-type (C14)
n=800 telomeres
average (p+q)= 43.42 ± 17.1 Kb.
p= 33.7 ± 11.6 Kb.
q= 53.1 ± 16.1 Kb.
free-ends= 0%
Lck-Tert (C15)
n= 1120 telomeres
average (p+q)= 50.1 ± 18.1 Kb.
p= 40.3 ± 13.9 Kb.
q= 59.9 ± 16.4 Kb.
free-ends= 0%
Lck-Tert (C15)
n=800 telomeres
average (p+q)= 45.0 ± 15.4 Kb.
p= 37.3 ± 10.4 Kb.
q= 52.7 ± 15.7 Kb.
free-ends= 0%
Frequency
Telomere length, Kb.

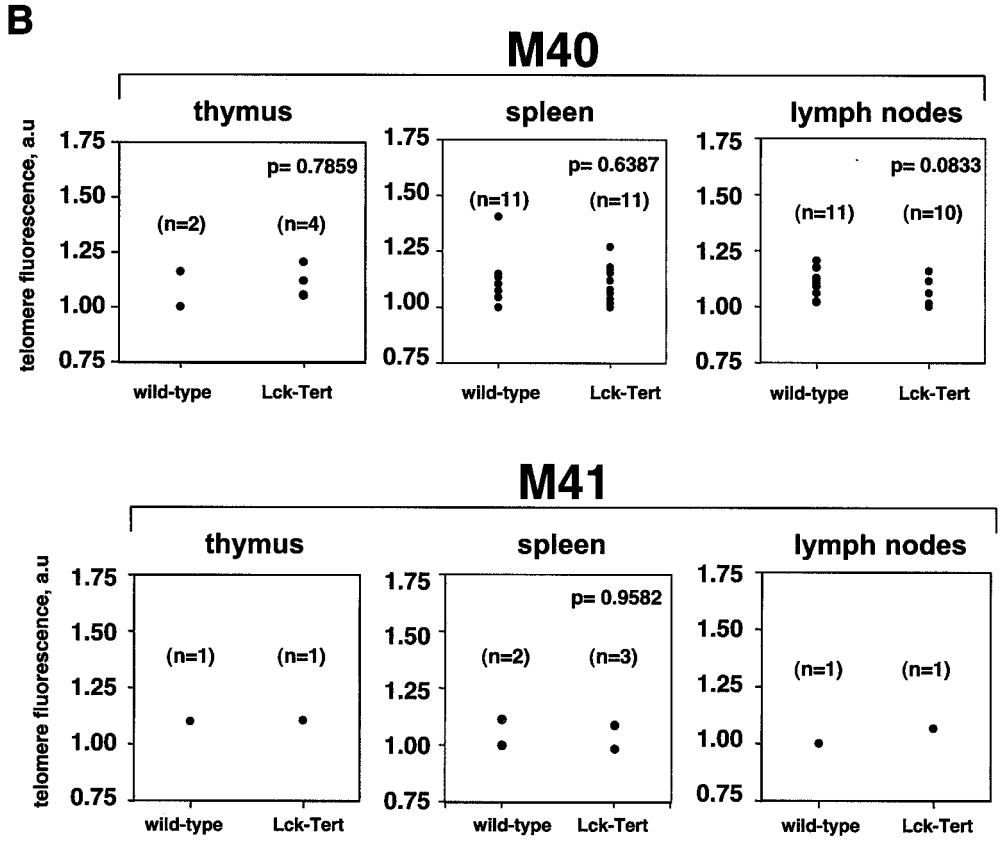

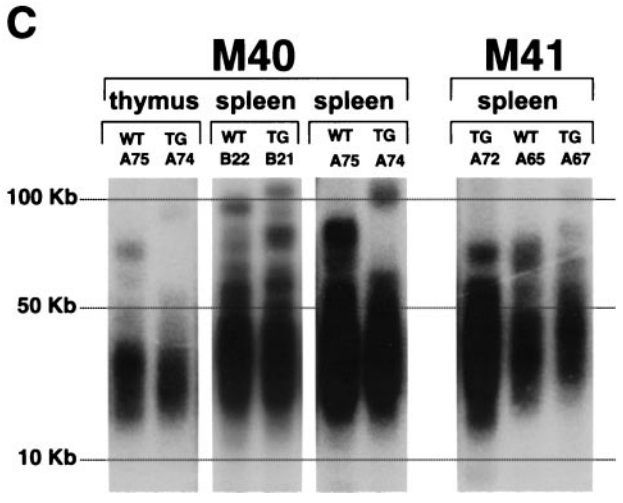

FIG. 3. Telomere lengths in lymphoid tissues from wild-type and Lck-Tert littermates from the indicated mouse lines. (A) Histograms showing telomere length frequencies in lymphocytes and lymph node cells derived from wild-type and Lck-Tert mice as determined by Q-FISH. The average lengths of p-arms, q-arms, and (p+q) arms are shown, together with the percentages of telomeres undetectable by Q-FISH (free ends) per metaphase. *n*, total number of telomeres included in each histogram. Mice D5 and D6 are littermates for which Q-FISH was performed in parallel, as are mice C14 and C15. All mice were derived from the M17 line. (B) Average telomere fluorescence, expressed in arbitrary units (a.u.), as determined by flow-FISH. The wild-type and Lck-Tert mice from each indicated line are littermates. *n*, number of mice used. (C) TRF analysis of lymphoid cells from Lck-Tert and wild-type littermates of the indicated lines. Designations of individual mice used in the analysis are given (A75, A74, etc.), and littermates are grouped together. TG, Lck-Tert; WT, wild type.

a consequence of telomerase overexpression, since telomerase has been reported to act preferentially on critically short telomeres (19, 25). In turn, the shortest telomeres are critical for cell viability and chromosome stability (19, 25). The histograms of telomere length frequencies for primary thymocytes and lymph node cells from Lck-Tert and wild-type mice, however, showed no significant differences between genotypes (Fig. 3A). In particular, in both thymocytes and lymph node cells, the frequencies of short and undetectable telomeres (signal-free ends) are similar for Lck-Tert and wild-type mice (Fig. 3A). These results indicate that Tert overexpression does not alter the normal distribution of telomere lengths in Lck-Tert primary thymocytes.

We also measured telomere length in lymphoid tissues from Lck-Tert and wild-type littermates by using telomere flow-FISH, a technique that combines flow cytometry with telomere Q-FISH and that has been proven to be useful in determining telomere length in lymphoid cells (see Materials and Methods). Flow-FISH was performed on freshly isolated thymocytes, splenocytes, and lymph node cells from age-matched Lck-Tert mice and wild-type littermates of each of the indicated transgenic lines (Fig. 3B). In this case, 24-month-old animals were chosen for the analysis so as to detect any possible telomere length differences between genotypes with ag-

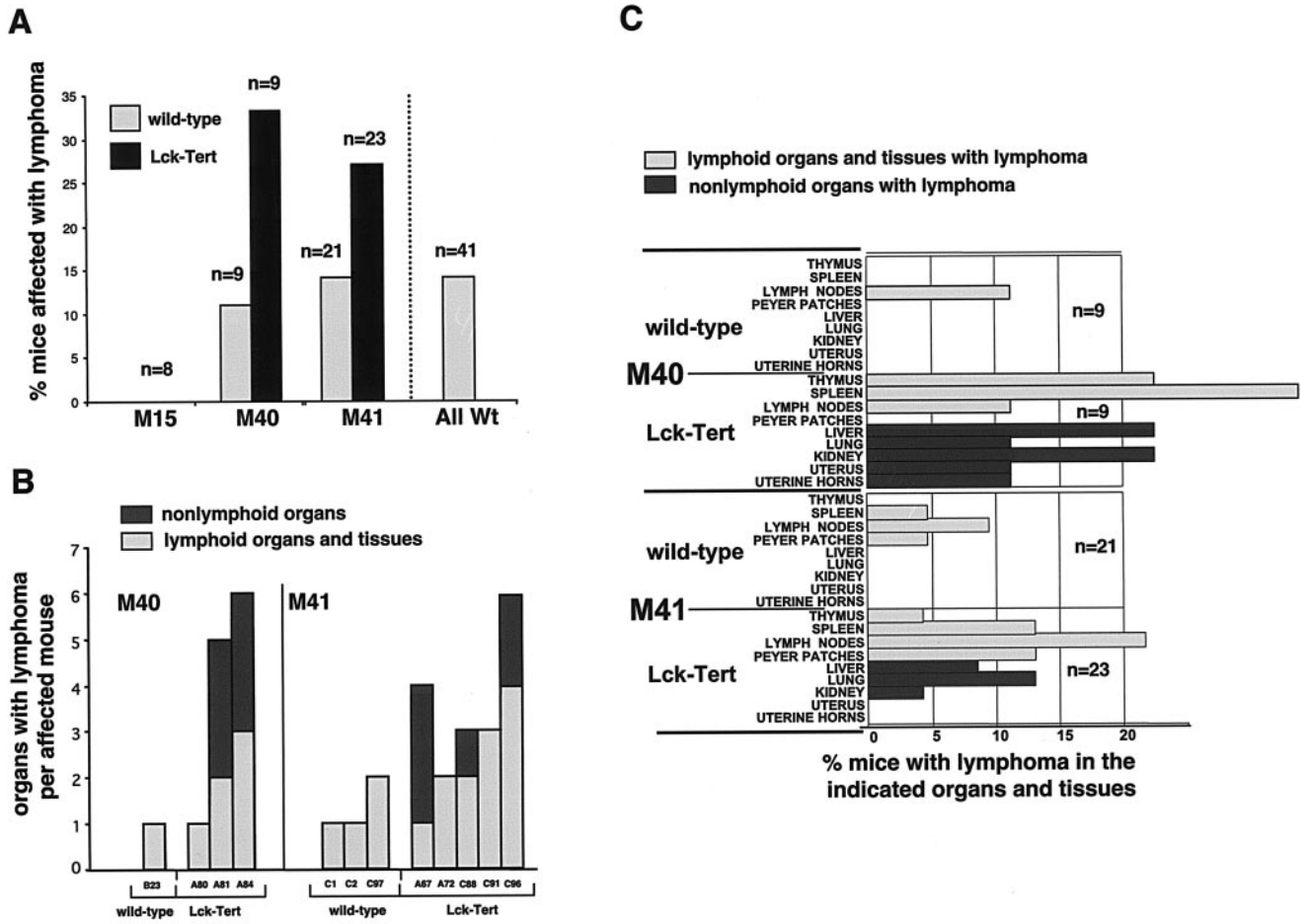

FIG. 4. Spontaneous-lymphoma incidence in 24-month-old wild-type and Lck-Tert mice. (A) Percentage of mice of each genotype affected with lymphoma in the indicated mouse lines. The average number of wild-type mice affected with lymphoma from the different transgenic lines is also shown in the "All Wt" category for comparison with Lck-Tert mice of the M15 line, which lacks wild types. *n*, number of mice. (B) Numbers of lymphoid and nonlymphoid organs with lymphoma in each of the affected Lck-Tert or wild-type mice whose designations are given at the bottom of the graph. (C) Percentage of mice of each genotype and mouse line that presented lymphoma in the indicated tissues. *n*, mice included in the analysis. A greater variety of both lymphoid and nonlymphoid tissues are affected with lymphoma in Lck-Tert mice than in wild-type controls. (D) Greater numbers of lymphoid and nonlymphoid organs showing lymphoma lesions and greater severity of lymphoma (scored according to the lymphoma severity index) in Lck-Tert mice than in wild-type controls of the M40 and M41 lines. Mice of the M15 line were excluded from the analyses because they do not express the transgene. Asterisks indicate statistically significant differences ($P \leq 0.05$ by Student's *t* test) between wild-type and Lck-Tert mice. The lymphoma severity index was determined for each mouse (see Materials and Methods). *n*, number of mice.

ing. Telomere fluorescence values for individual Lck-Tert and wild-type mice from the M40 and M41 mouse lines, however, showed no significant differences between genotypes, in agreement with the Q-FISH results ($P > 0.05$ by Student's *t* test in all cases) (Fig. 3B).

As an independent technique, not based on fluorescence, to estimate telomere length, we performed TRF analysis, which is based on visualization of telomeric DNA fragments by Southern blotting (see Materials and Methods). The average size of the TRF smear is indicative of the average telomere length. Again, no obvious differences in TRF product size were detected between Lck-Tert mice and wild-type littermates for any of the lymphoid tissues studied (Fig. 3C; littermates from the different genotypes are grouped for better comparison).

Taken together, these findings indicate that constitutive Tert expression in T cells from Lck-Tert mice does not result in a significant lengthening of telomeres compared to those from age-matched wild-type littermates. These results agree with those obtained for a different Tert transgenic mouse model, K5-Tert mice, with a telomere length similar to that of the corresponding wild-type controls (16). The absence of telomere lengthening in Lck-Tert cells agrees with the notion that telomerase preferentially elongates those telomeres that have lost telomere capping but does not result in further elongation of normal-length telomeres (19, 25).

Increased frequency of spontaneous lymphoma in Lck-Tert mice compared to that in age-matched wild-type littermates. To analyze the impact of Tert constitutive expression in T cells, we maintained large mouse colonies of the M15, M40, and M41 mouse lines (including both Lck-Tert mice and wild-type littermates) for at least 2 years (Table 1; Fig. 4). Lck-Tert mice of the M15 line were used as negative transgenic controls with null Lck-Tert mRNA expression. Age-matched (2-year-old) Lck-Tert and wild-type littermates of the different lines were

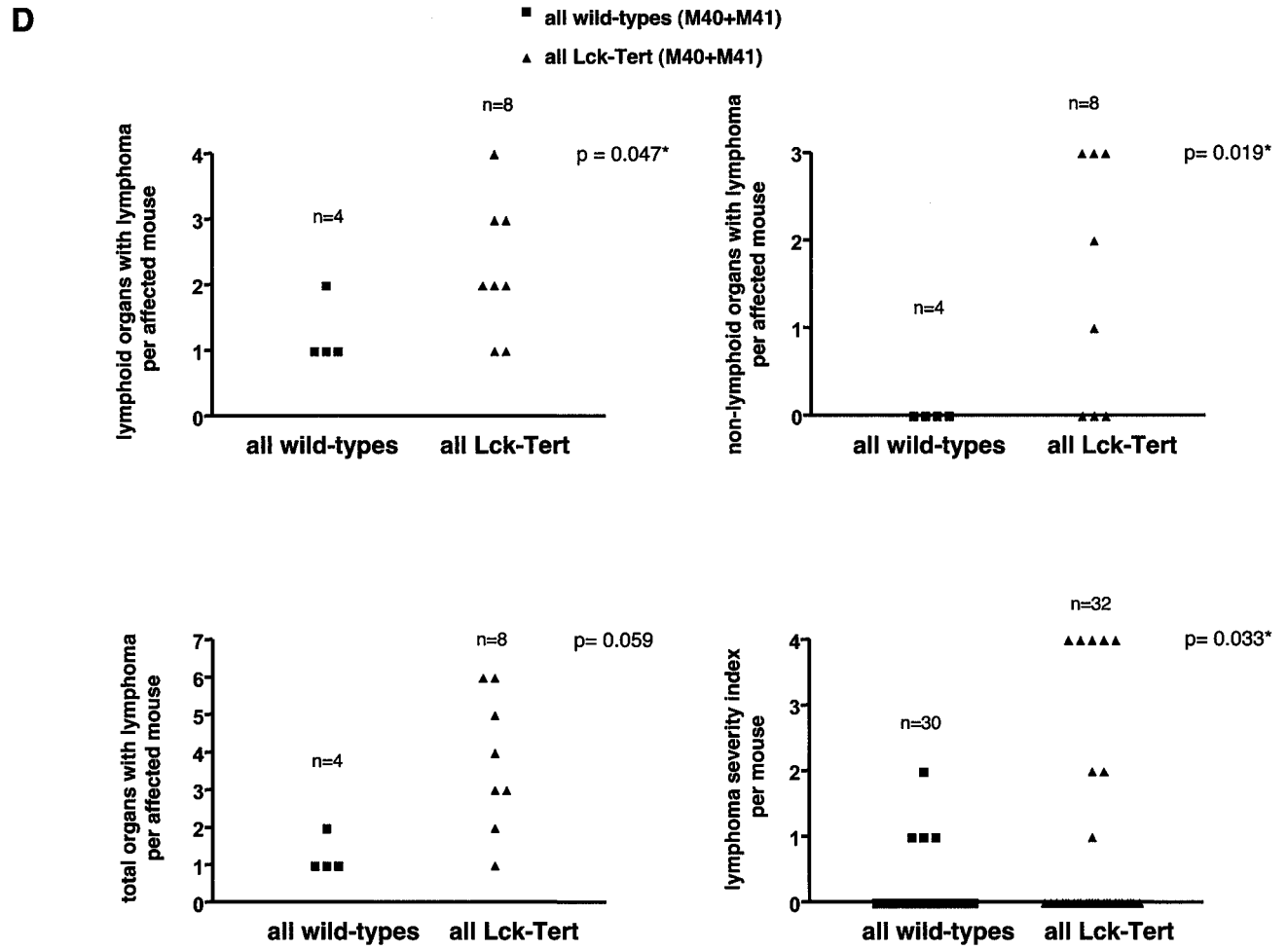

FIG. 4—*Continued.*

sacrificed in parallel and subjected to full-body histopathological analysis (see Materials and Methods). This approach allowed comparison of spontaneous tumor rates and tumor progression between age-matched Lck-Tert mice, which expressed (M40 and M41) or did not express (M15) transgenic Tert, and the corresponding wild-type littermate controls.

Neoplastic lesions were classified according to the cell type of origin and the type of lesion (Table 1). The percentage of mice that presented each type of lesion was determined for the different mouse lines and genotypes. Only the incidence of lymphomas was reproducibly higher in Lck-Tert mice than in their wild-type littermates; no differences were observed for

TABLE 1. Tumor spectrum in 24-month-old wild-type and Lck-Tert mice[a]

Cell type origin	Pathology	% of mice with the indicated tumor (no. of mice with tumor/total no. of mice)[b]					
		Total Wt (n = 42)	M15, Tg (n = 8)	M40		M41	
				Wt (n = 9)	Tg (n = 9)	Wt (n = 21)	Tg (n = 23)
Lymphocyte	Lymphoma	**14.2 (6/42)**	**0 (0/8)**	**11.1 (1/9)**	**33.3 (3/9)**	**14.2 (3/21)**	**21.7 (5/23)**
Liver	Hepatocellular adenoma	4.7 (2/42)	0 (0/8)	0 (0/9)	0 (0/9)	9.5 (2/21)	0 (0/23)
	Hepatocellular carcinoma	2.3 (1/42)	0 (0/8)	11.1 (1/9)	0 (0/9)	0 (0/21)	0 (0/23)
Lung	Bronchoalveolar adenoma	14.2 (6/42)	0 (0/8)	0 (0/9)	0 (0/9)	14.2 (3/21)	8.6 (2/23)
	Bronchoalveolar carcinoma	2.3 (1/42)	25 (2/8)	0 (0/9)	22.2 (2/9)	0 (0/21)	0 (0/23)
Thyroid	Thyroid follicular adenoma	2.3 (1/42)	0 (0/8)	0 (0/9)	0 (0/9)	0 (0/21)	4.3 (1/23)
Hypophysis	Hypophyseal adenoma	7.1 (1/42)	0 (0/8)	11.1 (1/9)	0 (0/9)	9.5 (2/21)	4.3 (1/23)
	Hypophyseal adenocarcinoma	0 (0/42)	0 (0/8)	0 (0/9)	11.1 (1/9)	0 (0/21)	0 (0/23)
Mammary glands	Mammary adenocarcinoma	0 (0/42)	0 (0/8)	0 (0/9)	11.1 (1/9)	0 (0/21)	0 (0/23)
Histiocyte	Histiocytic sarcoma	2.3 (1/42)	12.5 (1/8)	11.1 (1/9)	0 (0/9)	0 (0/21)	4.3 (1/23)

[a] See Fig. 4D for statistical analysis of lymphoma incidence and dissemination.
[b] Boldfacing indicates significant differences between wild-type (Wt) and transgenic (Tg) mice.

A

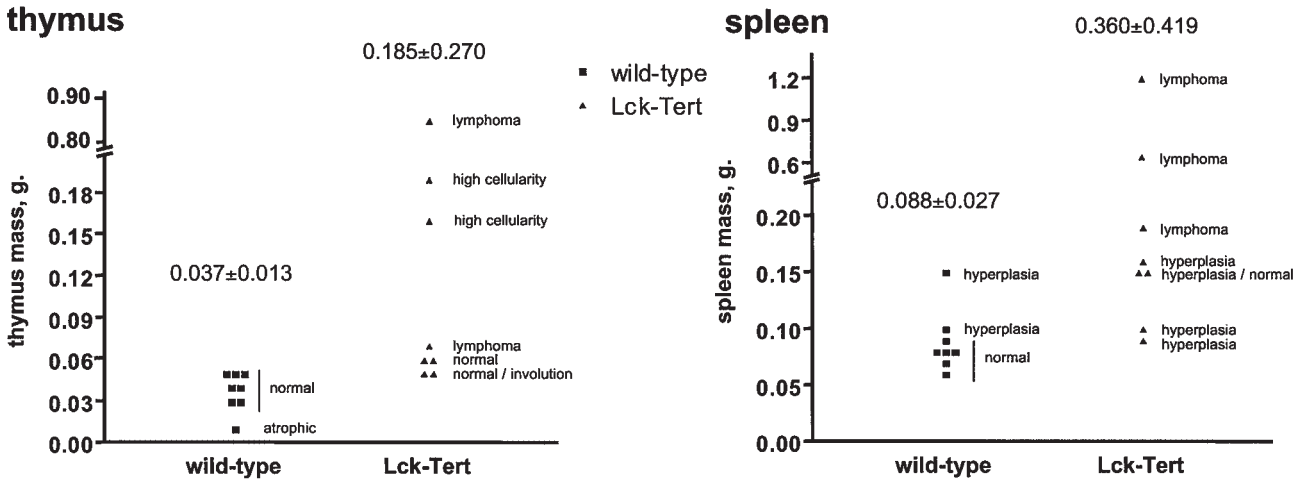
thymus
0.185±0.270
wild-type
Lck-Tert
lymphoma
high cellularity
high cellularity
lymphoma
normal
normal / involution
0.037±0.013
normal
atrophic
thymus mass, g.
0.90
0.80
0.18
0.15
0.12
0.09
0.06
0.03
0.00
wild-type
Lck-Tert
spleen
0.360±0.419
lymphoma
lymphoma
lymphoma
hyperplasia
hyperplasia / normal
0.088±0.027
hyperplasia
hyperplasia
normal
hyperplasia
hyperplasia
spleen mass, g.
1.2
0.9
0.6
0.20
0.15
0.10
0.05
0.00
wild-type
Lck-Tert

B

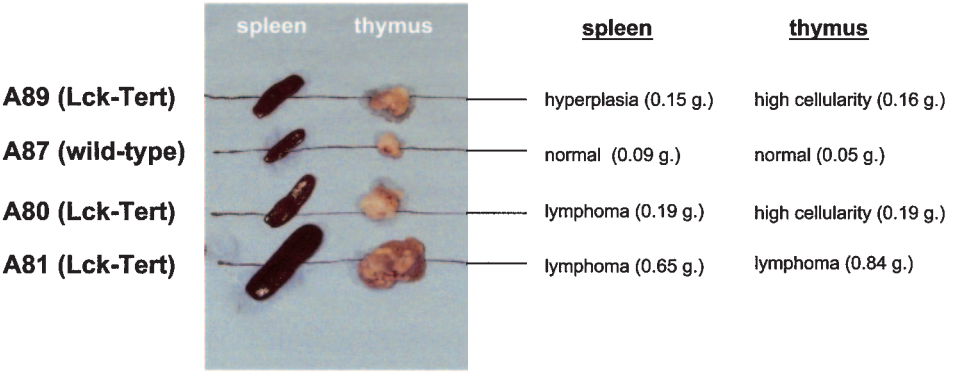
spleen
thymus
spleen
thymus
A89 (Lck-Tert)
hyperplasia (0.15 g.)
high cellularity (0.16 g.)
A87 (wild-type)
normal (0.09 g.)
normal (0.05 g.)
A80 (Lck-Tert)
lymphoma (0.19 g.)
high cellularity (0.19 g.)
A81 (Lck-Tert)
lymphoma (0.65 g.)
lymphoma (0.84 g.)

C

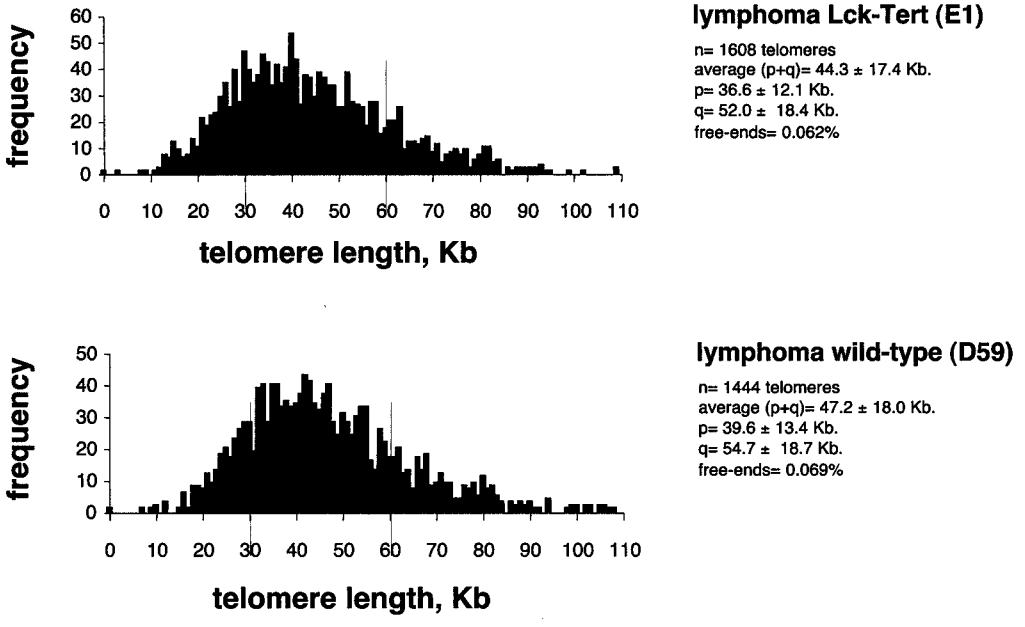
frequency
60
50
40
30
20
10
0
0 10 20 30 40 50 60 70 80 90 100 110
telomere length, Kb
lymphoma Lck-Tert (E1)
n= 1608 telomeres
average (p+q)= 44.3 ± 17.4 Kb.
p= 36.6 ± 12.1 Kb.
q= 52.0 ± 18.4 Kb.
free-ends= 0.062%
frequency
50
40
30
20
10
0
0 10 20 30 40 50 60 70 80 90 100 110
telomere length, Kb
lymphoma wild-type (D59)
n= 1444 telomeres
average (p+q)= 47.2 ± 18.0 Kb.
p= 39.6 ± 13.4 Kb.
q= 54.7 ± 18.7 Kb.
free-ends= 0.069%

other tumor types (see Fig. 4D for statistical calculations). The incidence of bronchoalveolar carcinoma was increased in Lck-Tert mice of the M15 and M40 lines compared with that for their wild-type littermates; however, this lesion did not coincide with Lck-Tert mRNA expression (i.e., the lesion is present in M15 Lck-Tert mice, which do not express transgenic Lck-Tert mRNA [Fig. 1B]) and thus is not a direct consequence of Tert constitutive expression. In contrast, increased lymphoma incidence was observed in Lck-Tert mice of the M40 and M41 lines, with high transgene expression, but not in the M15 line, which did not express the transgene. In particular, 21.7 and 14.2% of Lck-Tert and wild-type mice, respectively, were affected with lymphoma in the M41 line; for the M40 line, these percentages were 33.3 and 11.1%, respectively (Table 1; Fig. 4A). In addition, most of the lymphomas present in Lck-Tert mice were macroscopic at the time of sacrifice, while lymphomas in wild-type mice could be diagnosed only after histopathological analysis (see Fig. 5A and B for thymus and spleen sizes, as well as for histopathological diagnoses, of wild-type and Lck-Tert mice of the M40 line at the time of sacrifice). None of the Lck-Tert mice of the M15 line, which were null for transgene expression, showed spontaneous lymphoma, compared with an average of 14.2% of wild-type mice (Table 1; Fig. 4A). In addition, wild-type and Lck-Tert mice from the M40 line were left to age in the animal facility in order to study spontaneous-lymphoma incidence at the time of death. In agreement with the results obtained for mice sacrificed at the age of 2 years, 33.3% of Lck-Tert mice showed macroscopic lymphoma lesions at the time of death, compared to only 18% of the wild-type controls. Importantly, telomere lengths were similar in tumor cells isolated from wild-type and Lck-Tert T-cell lymphomas (see Fig. 5C), suggesting that the increased lymphoma incidence in Lck-Tert mice is not the consequence of longer telomeres in lymphoma cells in these mice.

In summary, an increase in spontaneous-lymphoma incidence was detected in two independent lines of Lck-Tert mice over that in age-matched wild-type controls or in the M15 Lck-Tert line, with null transgene expression. Lymphomas were the only tumor type whose incidence was increased in Lck-Tert mice compared to wild-type mice; no reproducible differences in the incidences of other tumor types were observed between genotypes (Table 1). These findings suggest that constitutive Tert expression targeted to T cells specifically promotes lymphoma in the context of the organism in the absence of significant differences in telomere length and in agreement with the specific pattern of Tert overexpression.

We also studied whether transgenic Tert expression in Lck-Tert mice resulted in abnormal blood cell counts in these mice. For this purpose, we analyzed peripheral blood in Lck-Tert and wild-type mice at the age of 22 to 27 weeks (Table 2). We reproducibly detected slight increases in the numbers of white blood cells and lymphocytes (leukocytosis and lymphocytosis) in Lck-Tert mice over those in wild-type controls (Table 2); however, these differences were not statistically significant ($P = 0.18$ by the chi-square test). Similarly, we detected no differences in red blood cell counts or the blood formula between genotypes (Table 2). In addition, we found no detectable organ damage or pathology in these Lck-Tert mice that could be related to abnormal T-cell counts. In particular, no significant differences in the incidence of glomerulonephritis or other autoimmune diseases, associated with abnormal lymphocyte proliferation and accumulation, were detected between genotypes (data not shown).

TABLE 2. Hematology analyses of wild-type and Lck-Tert mice

Cell type or parameter and condition[a]	No. (%) of mice with the indicated condition	
	Lck-Tert ($n = 10$)	Wild type ($n = 11$)
Leukocytes		
Leukocytosis[b]	5 (50)	2 (18.1)
Leukopenia	1 (10)	2 (18.1)
Normal	4 (40)	7 (63.6)
Lymphocytes		
Lymphocytosis	5 (50)	4 (36.3)
Lymphopenia	2 (20)	3 (27.2)
Normal	3 (30)	4 (36.3)
Granulocytes		
Granulocytosis	1 (10)	
Normal	9 (90)	11 (100)
Blood formula[c]		
Altered	4 (40)	4 (36.3)
Normal	6 (60)	7 (63.6)
Red blood cells[d]		
Polycytemia		1 (9)
Anemia	1 (10)	1 (9)
Normal	9 (90)	9 (81.8)

[a] See Materials and Methods for reference values.
[b] Abnormal white blood cell counts (leukocytosis) were generally accompanied by abnormal lymphocyte counts (lymphocytosis).
[c] Reflects the relative proportion between lymphocytes and granulocytes. No differences in the frequency of altered blood formula were detected between genotypes.
[d] No differences in the frequency of altered red blood cell counts were detected between genotypes.

Transgenic telomerase increases the dissemination of Lck-Tert lymphoma to both lymphoid and nonlymphoid tissues. Histopathological analysis of all the spontaneous-lymphoma cases showed increases in total numbers of both lymphoid and nonlymphoid organs (Fig. 4B; for examples, see Fig. 5A and B and Fig. 6A through C) affected with lymphoma in LcK-Tert mice compared to those in wild-type controls. Figure 4D shows significant increases in the numbers of both lymphoid and nonlymphoid organs affected with lymphoma in Lck-Tert mice when all Lck-Tert mice that developed lymphoma in lines M40 and M41 are compared with all wild-type controls. In particular, a larger variety of lymphoid tissues per mouse were affected with lymphoma in Lck-Tert mice than in wild-type con-

FIG. 5. (A) Quantification of thymus and spleen weights (corrected by body size), with histopathological diagnosis, for each 2-year-old wild-type and Lck-Tert mouse of the M40 line. The average organ weight and standard deviation for each genotype is shown above the scatter distributions. (B) Representative images and histopathological diagnoses of thymuses and spleens from wild-type and Lck-Tert mice (littermates) at the age of 2 years. Mouse designations are given on the left. All mice are from the same litter. (C) Telomere length distributions as determined by Q-FISH in tumor cells isolated from wild-type and Lck-Tert lymphomas. Average lengths of p-telomeres, q-telomeres, and (p+q) telomeres are given, together with the percentages of undetectable telomeres (free ends) per metaphase. *n*, total number of telomeres included in each histogram.

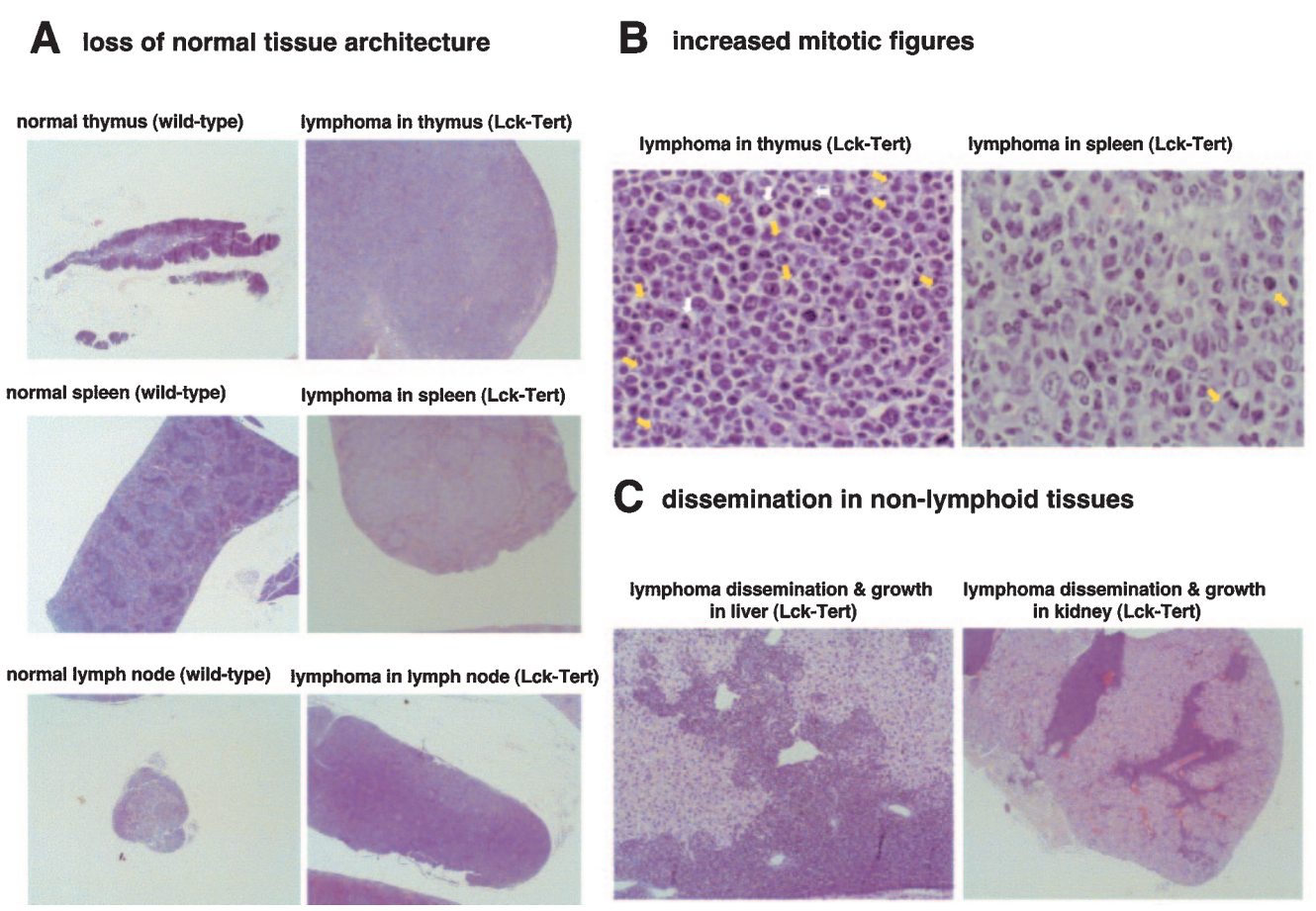

FIG. 6. Criteria used to identify lymphoma lesions and to distinguish them from lymphoproliferative pathology. (A) Loss of normal architecture in lymphoma-affected tissues compared to corresponding normal healthy tissues. The normal thymus is composed of cortex and medulla; the lymphoma-affected thymus is enlarged, has lost its normal differentiation, and is composed of a uniform population of cells. In the normal spleen, there is a clear separation between the white pulp (lymphoid tissue) and the red pulp. In the lymphoma-affected spleen, there is a progressive expansion of follicles in the white pulp, with compression of the red pulp and the periarteriolar sheaths. The normal lymph node is composed of cortex and medulla. In the lymphoma-affected lymph node, there is a loss of normal architecture and infiltration of neoplastic lymphocytes in the medulla, capsula, and adjacent connective tissue. (B). With lymphoma in the thymus, there is an increase in the number of mitotic figures (yellow arrows) and the presence of a pleomorphic population of lymphoblasts showing many mitotic figures (yellow arrows) with moderate apoptosis (white arrows). With lymphoma in the spleen, there is a population of large centroblasts, centrocytes, and small lymphocytes obliterating normal architecture. Numerous mitotic figures can be detected (arrows). (C) Examples of infiltration and growth of lymphoma in the liver (extensive periportal and subcortical infiltration of malignant lymphoid cells) and the kidney (severe perivascular infiltration in the renal cortex, medulla, pelvis, and adjacent fat tissue). (D) Summary of lymphoma clonality results for the TCRβ, TCRγ, and IgH genes. A tumor was considered polyclonal (P) when a Gaussian distribution of multiple peaks (multiple PCR products) was obtained after capillary electrophoresis of the PCR. A tumor was considered monoclonal (M) when a single peak (only one PCR product) was obtained. In the case of coexistence with other peaks, a peak was considered monoclonal only if the peak area was >2-fold larger than the area of any other peak. A "weak monoclonal" (WM) profile was assigned when the area of the peak was 1.7- to 2-fold larger than the area of any other peak. n.p., no PCR product obtained. It should be noted that a sample was considered monoclonal when a monoclonal profile was obtained in at least one of the PCRs; it was not necessary that a monoclonal profile be obtained in all reactions. (E through G) Gene-scanning images after capillary electrophoresis of the indicated PCRs. Blue lines, PCR product. Red lines, DNA size marker. Product concentrations, in arbitrary fluorescence units, are shown along the *y* axis. Product sizes, in bases, are shown along the *x* axis.

trols (Fig. 4C and D; $P = 0.047$ by Student's *t* test). In addition, lymphoma in Lck-Tert mice not only affected lymphoid tissues (see Fig. 5A and B and Fig. 6A and B for examples) but also affected various nonlymphoid organs such as the liver (Fig. 6C), lungs, and kidney (Fig. 6C), which were never affected in the age-matched wild-type mice that developed lymphoma (see Fig. 4B through D for quantifications; $P = 0.019$ by Student's *t* test when all Lck-Tert mice of lines M40 and M41 that developed lymphoma are compared with all wild-type controls that developed lymphoma). It is noteworthy that infiltrating lymphomas were distinguished from lymphoproliferative disease based on Bethesda's proposed parameters (24). First, we evaluated organ architecture, cytology, and dissemination. As can be observed in Fig. 6, lymphoma lesions typically showed (i) loss of normal tissue architecture (Fig. 6A), (ii) monomorphic or pleiomorphic lymphoid cell populations containing numerous mitotic figures (Fig. 6B), and (iii) invasive dissemination of tumor cells in various lymphoid and nonlymphoid tissues (Fig. 6C). It is noteworthy that we also detected reactive expansions of lymphocytes, which were diagnosed as lymphoid

D

	TCRβ				TCRγ	IgH
	Vβ-Jβ1	Vβ-Jβ2	Dβ1-Jβ1	Dβ2-Jβ2	Vγ4-Jγ1	DSF-JH4
normal spleen	P	P	P	P	P	P
A80 spleen	M	M	P	M	P	M
A81 thymus	M	P	M	MW	M	P
A84 lymph nodes	M	P	M	M	P	P
A72 lymph nodes	M	M	P	P	MW	n.p.

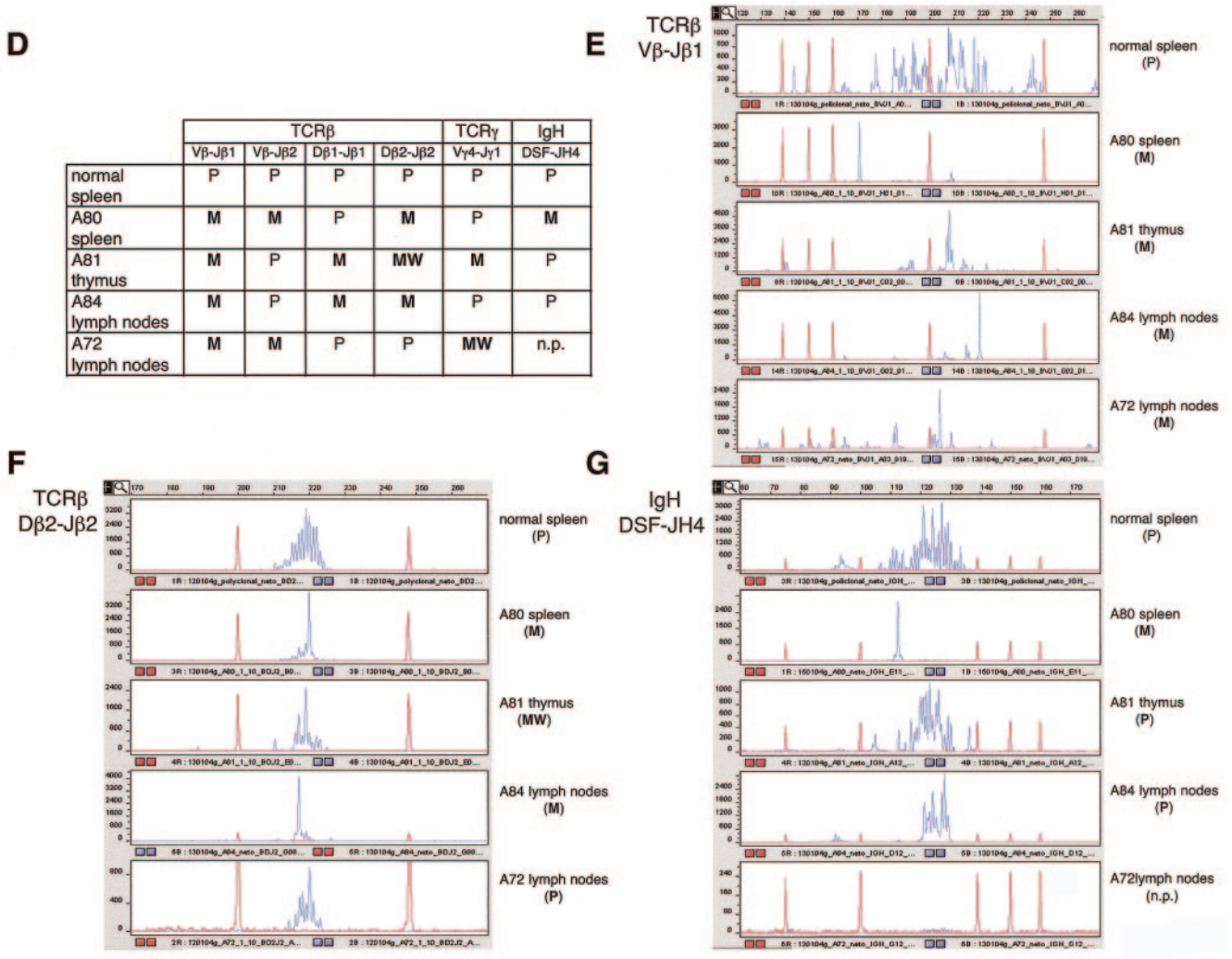

FIG. 6—*Continued.*

hyperplasias, in 2-year-old mice (see Fig. 5A through C for examples); however, no significant differences between genotypes were observed in this pathology (data not shown).

Next, we examined the clonal nature (clonality) of lymphomas appearing in Lck-Tert mice, an important parameter for distinguishing between lymphoproliferative disorders and lymphoma (24). In particular we studied clonality for three different genes: TCRβ, TCRγ, and IgH (Fig. 6D through G). For this purpose, we used specific sets of primers and performed PCR analysis of genomic DNA derived from lymphoma-affected organs (see Materials and Methods). In particular, we used a set of primers for TCRβ that amplifies rearrangements in Vβ-DJβ and Dβ-Jβ gene segments (13), a set of primers for TCRγ that amplifies rearrangements of Vγ-Dγ gene segments (13), and a set of primers for IgH that amplifies rearrangements of DH-JH gene segments (21). All Lck-Tert lymphomas showed a clear monoclonal profile for the TCRβ gene (Fig. 6D through F), and two out of four Lck-Tert lymphomas were monoclonal for TCRγ (Fig. 6D). In addition, one out of four Lck-Tert lymphomas was monoclonal for IgH as well as monoclonal for TCRβ (Fig. 6D and G). Simultaneous monoclonality for IgH and TCRβ has been described for a small proportion of T-cell malignancies (24). Taken together, these results indicate a clear monoclonal character for Lck-Tert lymphomas, reinforcing the notion that Lck-Tert mice develop malignant T-cell lymphoma rather than a lymphoproliferative disorder (24). In addition, the remarkable TCRβ monoclonality of Lck-Tert lymphomas emphasizes their clear T-cell origin.

To evaluate differences between genotypes in the incidence and severity of lymphomas, we calculated a score on the lymphoma severity index for each mouse included in the study (see Materials and Methods) (Fig. 4D). Lck-Tert mice showed significantly higher lymphoma severity index scores than wild-type controls (Fig. 4D; $P = 0.033$ by Student's t test upon comparison of severity index scores of all Lck-Tert and wild-type littermates from lines M40 and M41).

Taken together, these results show that lymphomas appearing in Lck-Tert mice are more aggressive than those in wild-type controls, as indicated by significant increases in the numbers and varieties of lymphoid and nonlymphoid organs affected with lymphoma. These results suggest that Tert overexpression confers a more malignant phenotype on murine

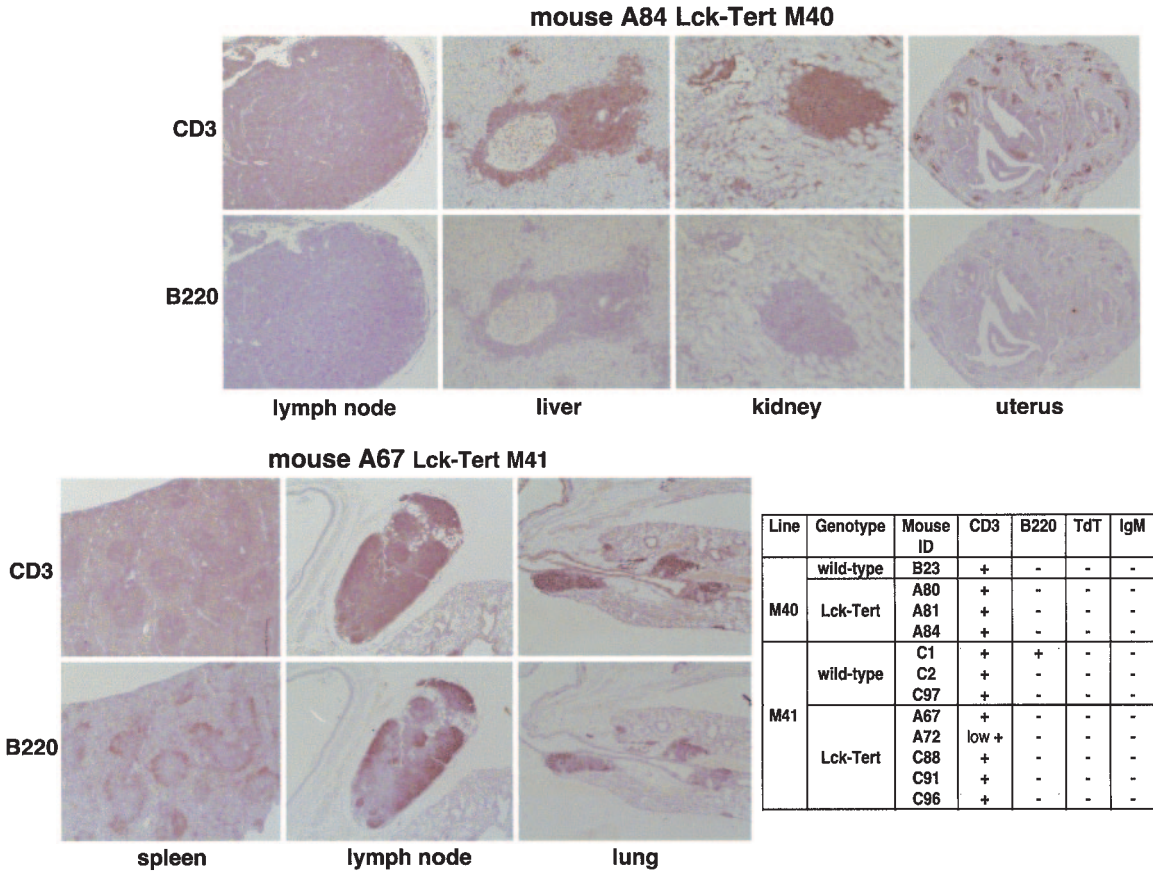

Line	Genotype	Mouse ID	CD3	B220	TdT	IgM	FACS
M40	wild-type	B23	+	-	-	-	normal
	Lck-Tert	A80	+	-	-	-	CD3+ CD4+ CD8- B200-
		A81	+	-	-	-	CD3+ CD4- CD8- B220-
		A84	+	-	-	-	CD3+ CD4- CD8+ B220-
M41	wild-type	C1	+	+	-	-	n.d.
		C2	+	-	-	-	n.d.
		C97	+	-	-	-	n.d.
	Lck-Tert	A67	+	-	-	-	n.d.
		A72	low +	-	-	-	CD3lo CD4lo CD8lo B220-
		C88	+	-	-	-	n.d.
		C91	+	-	-	-	n.d.
		C96	+	-	-	-	n.d.

FIG. 7. Lymphomas were characterized by immunohistochemistry using anti-CD3, anti-B220, anti-TdT, and anti-IgM antibodies, as well as by FACS analysis using anti-CD3, anti-CD4, anti-CD8, and anti-B220 antibodies. (Top and bottom left) Representative images of anti-CD3 and anti-B220 staining of tissues affected with lymphoma from individual Lck-Tert mice (A84 and A67). (Bottom right) Table shows that the lymphoma lesions present in Lck-Tert mice are predominantly positive for CD3 and negative for B220, IgM, and TdT, suggesting a mature T-cell origin for Lck-Tert lymphomas. The table also gives FACS analysis data. n.d., not determined; lo, low positivity.

lymphoma progression, revealing a novel role of telomerase in sustaining tumor dissemination.

Spontaneous lymphomas in transgenic mice are predominantly of a mature T-cell origin. If constitutive Tert expression in T cells was responsible for promoting malignant lymphoma in Lck-Tert mice, we should expect the nonlymphoid tissues affected with lymphoma to be highly positive for T-cell markers, such as CD3 staining, but negative for B-cell markers such as B220 and IgM staining. To investigate this question, we first performed immunohistochemistry with anti-CD3, anti-B220, and anti-IgM antibodies on various tissues affected with lymphoma from individual Lck-Tert mice of both the M40 and M41 lines. In addition, to determine whether the lymphomas had a mature origin, we performed immunohistochemistry with an anti-TdT antibody, since TdT is a marker of precursor T- and B-cell lymphomas. The spontaneous-lymphoma lesions present in different tissues from Lck-Tert mice were predominantly positive for the CD3 marker and negative for B220 and IgM, suggesting that they had originated mostly from T cells (Fig. 7). For wild-type mice, some of the lymphoma lesions were predominantly positive for B220 staining (Fig. 7), suggesting that they had originated mostly from B cells. Furthermore, the negative staining for the anti-TdT antibody in all Lck-Tert lymphomas suggests a mature T-cell origin for these lymphomas (Fig. 7).

We confirmed these findings by performing FACS analysis on some of the Lck-Tert lymphomas by using anti-CD4, anti-CD8, anti-B220, and anti-CD3 antibodies. FACS analysis showed that Lck-Tert lymphomas were CD3 positive, B220 negative, and predominantly single positive for the anti-CD4 or anti-CD8 antibody ($CD4^+$ $CD8^-$ or $CD4^-$ $CD8^+$), again suggesting their mature T-cell origin (Fig. 7). In summary, both immunohistochemistry and FACS analyses suggest that Lck-Tert lymphomas are predominantly mature T-cell lymphomas.

T-cell lymphomas in Lck-Tert mice preserve Lck-Tert expression at a higher rate than corresponding normal Lck-Tert tissues. We next studied whether T-cell lymphomas in Lck-Tert mice preserved transgenic Tert expression. For this purpose, we performed real-time RT-PCR using primers that amplify endogenous or transgenic Tert (A primers or hGHp2 primers, respectively). Most of the lymphoma lesions present in various organs from Lck-Tert mice showed increased Tert mRNA expression levels with A primers compared to those in the corresponding normal Lck-Tert tissues; a ratio of 1 indicates similar Tert mRNA expression in normal and lymphoma tissues (Fig. 8A). Therefore, Tert expression is preserved or

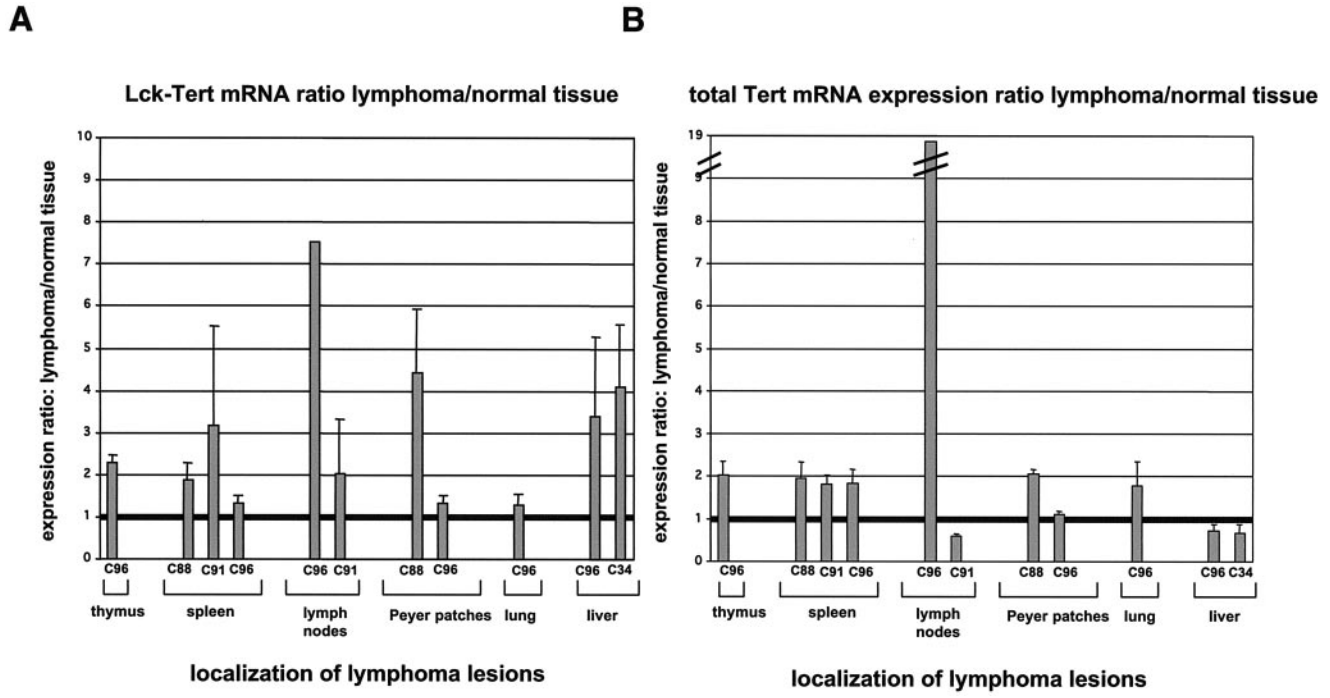

FIG. 8. Real-time quantitative RT-PCR analysis of both Lck-Tert mRNA and total Tert mRNA expression in Lck-Tert lymphomas. (A) Lck-Tert mRNA was quantified by using hGHp2 primers. Histogram shows the ratio of Lck-Tert expression between lymphomas and corresponding normal Lck-Tert tissues. (B) Total Tert mRNA was quantified by using A primers. Histogram shows the ratio of Tert mRNA expression between lymphomas and corresponding normal Lck-Tert tissues. A ratio of 1 indicates equal mRNA expression in normal and lymphoma-affected Lck-Tert tissues. Most Lck-Tert lymphomas showed higher transgenic Tert expression than normal Lck-Tert tissues, supporting the Lck-Tert origin of these lesions. Designations of the Lck-Tert mice with lymphoma lesions used for the analysis are given below the graphs.

increased in lymphoma lesions relative to expression in corresponding normal tissues in Lck-Tert mice. Similarly, when Lck-Tert-specific primers were used, transgenic Tert mRNA levels were increased in most lymphoma lesions present in Lck-Tert mice compared with those in the corresponding normal Lck-Tert tissues (Fig. 8B), as would be expected if these lymphoma lesions were mostly derived from Lck-Tert-expressing T cells.

Normal telomere capping but increased chromosomal damage in Lck-Tert thymocytes compared to wild-type controls. To investigate the mechanisms by which Tert constitutive expression could be promoting T-cell lymphoma in Lck-Tert mice independently of the known role of telomerase in net telomere elongation, we first studied whether primary thymocytes derived from Lck-Tert mice showed a normal telomere capping function. It is plausible that an excess of Tert in Lck-Tert thymocytes could interfere with the formation of a proper telomere cap in these cells. A hallmark of defective telomere capping is a higher incidence of spontaneous end-to-end chromosome-type and chromatid-type fusions involving telomeric sequences (2, 7, 17). In the mouse, the most frequent type of end-to-end fusion associated with telomere dysfunction is RLF (7, 17). In addition, it has recently been shown that loss of telomere capping interferes with proper repair of DNA double-strand breaks (DSB) in the genome, as indicated by the fact that telomerase-deficient mice with critically short or uncapped telomeres are hypersensitive to ionizing radiation (IR) (18, 22, 32). In particular, critically short telomeres in these mice illegitimately join to IR-induced DSB in the genome, thus increasing chromosomal instability (22). Furthermore, there has been recent speculation that Tert overexpression may directly interfere with proper DNA repair of lesions in the genome in a way that is independent of telomere capping (5).

To address these possibilities, we performed a full karyotypic analysis of ~100 metaphases of primary thymocytes isolated from both wild-type and Lck-Tert mice of two independent mouse lines (M17 and M40) before or after whole-body IR with a single dose of gamma rays (4 Gy) (see Materials and Methods). In the absence of IR, Lck-Tert thymocytes showed increased frequencies of chromatid breaks and TA compared to those for the corresponding nonirradiated wild-type controls (Table 3; Fig. 9A; for examples of aberrations, see Fig. 9B). However, we did not detect significantly increased frequencies of end-to-end fusions involving the telomeres (Robertsonian-like fusions [RLF] plus multicentrics plus rings) in Lck-Tert thymocytes compared to those in controls (Table 3; Fig. 9A). Significantly, no RLF or dicentrics were detected in nonirradiated Lck-Tert thymocytes from two different Lck-Tert mouse lines (M17 and M40) (Table 3; Fig. 9A), indicating that telomere function was intact in these cells and that, therefore, overexpressed Tert does not interfere with the formation of a proper telomere capping structure.

Upon gamma irradiation, Lck-Tert thymocytes from two independent mouse lines (M17 and M40) showed significantly increased frequencies of fusions (particularly dicentrics and tricentrics) and fragments compared to those for similarly irradiated wild-type controls (Table 3; Fig. 9A; see Fig. 9B for

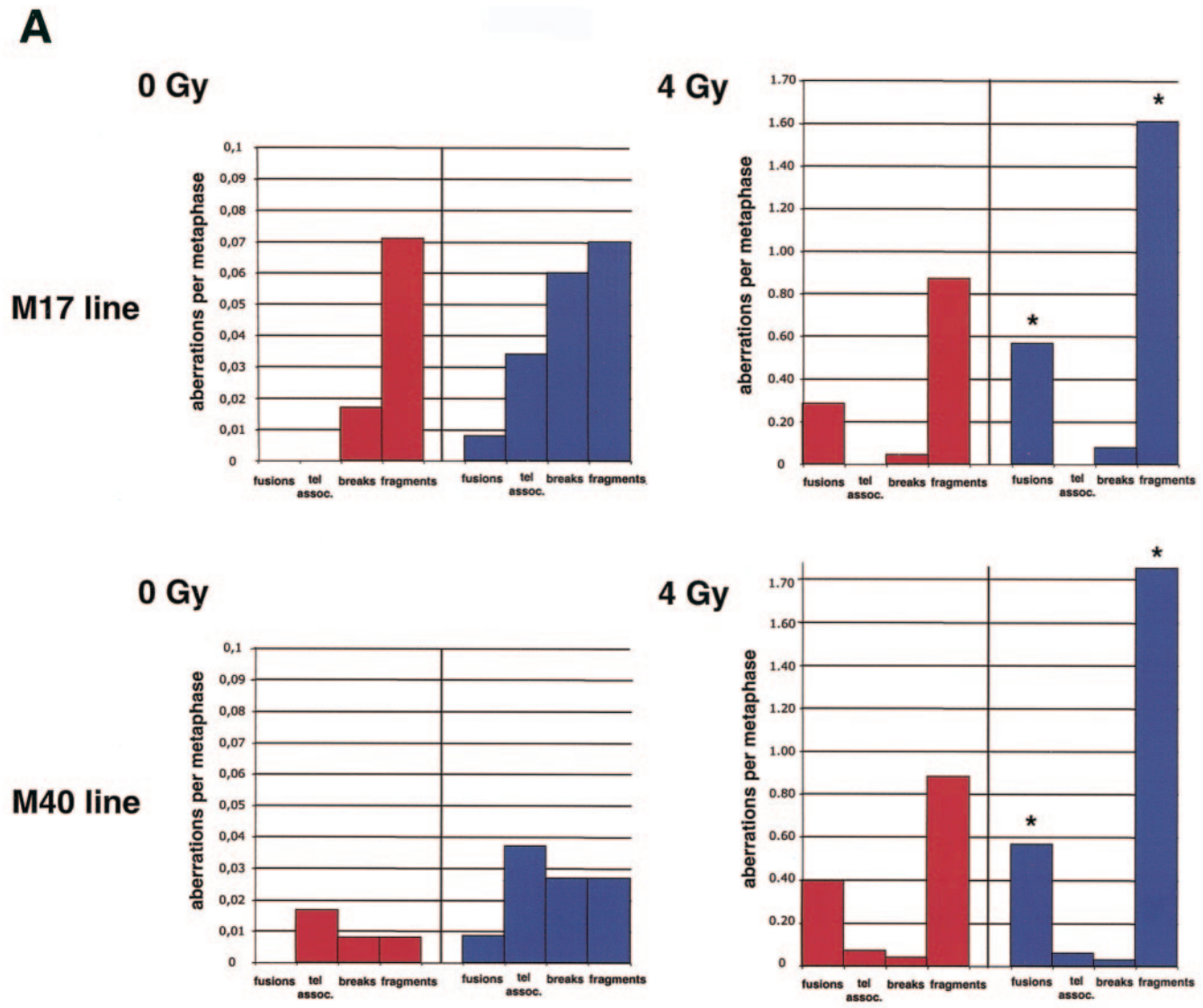

FIG. 9. (A) Frequencies of chromosomal aberrations per metaphase. Lck-Tert (blue bars) and wild-type (red bars) thymocytes from two independent mouse lines (M17 and M40) were analyzed in the absence of IR (0 Gy) or after IR (4 Gy). Asterisks indicate highly significant differences between irradiated Lck-Tert and wild-type mice ($P < 0.05$). (B) Representative examples of the indicated chromosomal aberrations detected by telomeric Q-FISH (see Materials and Methods). Blue, 4′,6′-diamidino-2-phenylindole (DAPI); yellow, TTAGGG repeats. RT-like, RLF; chrom., chromosome; frag., fragment.

representative examples). However, these fusions never showed telomeric TTAGGG repeats at the fusion, again indicating proficient telomere capping.

Altogether, Lck-Tert thymocytes show greater spontaneous and IR-induced chromosomal instability than wild-type controls. In addition, a higher percentage of metaphases showed chromosomal aberrations in Lck-Tert thymocytes than in wild-type controls (Table 3). However, the fact that telomeric sequences are not involved in these aberrations indicates that Tert overexpression does not directly interfere with proper telomere capping; instead, Tert overexpression may interfere with DNA repair of DSB in the genome or with the cellular response to DNA damage.

DISCUSSION

Telomerase is essential for conferring indefinite growth potential on tumor cells through its ability to elongate short telomeres, which otherwise could trigger loss of cell viability (4, 27). This role led to the proposition that in the absence of telomerase, short telomeres can act as tumor suppressors, thus encouraging the use of telomerase inhibitors as potential anticancer drugs in combination with other chemotherapeutic or radiotherapeutic agents (4, 6, 15, 27). However, the efficiency of telomerase inhibitors in cancer treatment may be higher than initially predicted. In particular, recent evidence indicates a novel role for telomerase in promoting growth and tumori-

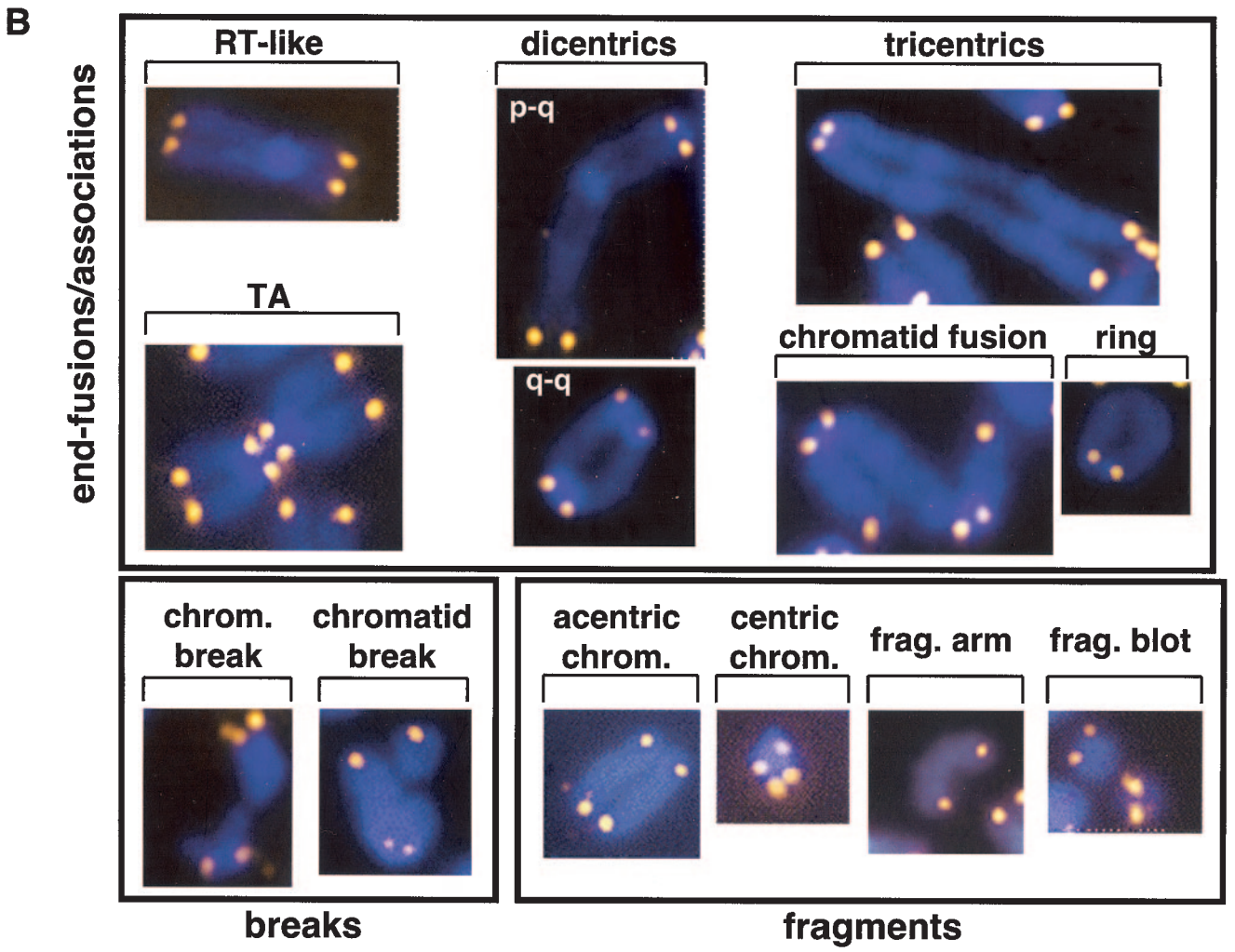

FIG. 9—*Continued.*

genesis, independent of its role in telomere elongation (5). In particular, mice with transgenic Tert expression have a higher incidence of tumors than wild-type mice showing similar telomere lengths (1, 14, 16). In addition, evidence obtained using cultured cells also supports a role of telomerase in promoting growth and survival independent of its role in net telomere elongation (28, 29). This role of telomerase in promoting tumorigenesis is of particular relevance for cancer treatment, since it implies that a putative telomerase inhibitor would be effective in delaying tumor growth even when telomeres have not yet reached a critically short length (5, 6). However, more studies using mouse models are needed to understand the effects of Tert overexpression in the context of the organism, since these effects may largely vary depending on the cell type.

We have generated a new mouse model, Lck-Tert mice, with constitutive Tert expression specifically targeted to thymocytes and peripheral T cells, which provides strong evidence for additional roles of Tert in promoting tumorigenesis. In particular, Lck-Tert mice from two independent transgenic lines, M40 and M41, have higher incidences of T-cell lymphoma, but not of other tumor types, than age-matched wild-type littermates. Importantly, we demonstrate here that the increased incidence of T-cell lymphoma is specific to Lck-Tert mRNA expression and is not due to nonspecific effects of transgene integration, as indicated by the fact that it occurs in two independent lines, M40 and M41, with high Lck-Tert mRNA expression but does not occur in the M15 Lck-Tert line, with no detectable Lck-Tert mRNA expression. An advantage of having generated mice with Tert specifically targeted to thymocytes and T cells is that these cell types allow us to measure telomere length in metaphase spreads from primary thymocytes freshly isolated from these mice. The Q-FISH results indicate that the telomeres of Lck-Tert mice that overexpress Tert are similar in length to those of wild-type controls. Therefore, constitutive high telomerase expression in T cells promotes spontaneous T-cell lymphoma in a manner that is uncoupled from the role of telomerase in net telomere elongation. Altogether, these results provide strong evidence that Tert promotes tumorigenesis independently of telomere length changes.

Besides providing new evidence on the role of telomerase in promoting tumorigenesis independently of telomere length,

TABLE 3. Chromosomal aberrations in primary thymocytes from irradiated or nonirradiated Lck-Tert and wild-type mice

Chromosomal aberration	Frequency per metaphase (total no. of aberrations) under the following conditions for the following mouse (mouse line)[a]							
	No IR				IR (4 Gy)			
	Wild type		Lck-Tert		Wild type		Lck-Tert	
	C14 (M17) (n = 110)	G43 (M40) (n = 112)	C15 (M17) (n = 113)	G45 (M40) (n = 105)	C86 (M17) (n = 58)	G51 (M40) (n = 101)	C85 (M17) (n = 47)	G48 (M40) (n = 101)
RLF	0	0	0	0	0	0.118 (12)	0.021 (1)	0.049 (5)
Dicentric p-q	0	0	0	0	0.017 (1)	0.049 (5)	**0.106 (5)**	**0.099 (10)**
Dicentric q-q	0	0	0	0	0.241 (14)	0.188 (19)	**0.404 (19)**	**0.316 (32)**
Tricentric p-q-q	0	0	0	0	0	0	0.021 (1)	0
Total dicentrics + tricentrics	0	0	0	0	0.258 (15)	0.237 (24)	**0.531 (25)**	**0.415 (42)**
Rings	0	0	**0.009 (1)**	**0.009 (1)**	0.034 (2)	0.049 (5)	0.021 (1)	**0.108 (11)**
RLF + multicentrics + rings	0	0	**0.009 (1)**	**0.009 (1)**	0.293 (17)	0.406 (41)	**0.574 (27)**	**0.574 (58)**
TA	0	0.017 (2)	**0.035 (4)**	**0.038 (4)**	0	0.079 (8)	0	0.069 (7)
Chromosome break	0	0	0.009 (1)	0	0	0.019 (2)	0.021 (1)	0
Chromatid break	0.018 (2)	0.0089 (1)	**0.053 (6)**	**0.028 (3)**	0.051 (3)	0.029 (3)	0.063 (3)	0.039 (4)
Total breaks	0.018 (2)	0.0089 (1)	**0.061 (7)**	**0.028 (3)**	0.051 (3)	0.049 (5)	0.085 (4)	0.039 (4)
Fragment (arm)	0.036 (4)	0	0.017 (2)	0	0.034 (2)	0	0.021 (1)	0.059 (6)
Fragment (blot)	0.027 (3)	0	0.035 (4)	0.028 (3)	0.620 (36)	0.564 (57)	**1.23 (58)**	**0.970 (98)**
Centric chromosome	0.009 (1)	0.0089 (1)	0.009 (1)	0	0.206 (12)	0.247 (25)	0.255 (12)	**0.514 (52)**
Acentric chromosome	0	0	0.009 (1)	0	0.017 (1)	0.079 (8)	**0.085 (4)**	**0.316 (32)**
Total fragments	0.072 (8)	0.0089 (1)	0.071 (8)	0.028 (3)	0.879 (51)	0.891 (90)	**1.595 (75)**	**1.861 (188)**
% of metaphases with aberrations	10%	3.5%	**13.2%**	**7.6%**	51.7%	57.4%	**63.8%**	**67.3%**

[a] n, number of metaphases analyzed. Boldfacing indicates that the frequency of aberrations was increased in Lck-Tert cells compared with that in wild-type cells.

the study of Lck-Tert mice also revealed a novel role of telomerase in sustaining invasive disease. In particular, T-cell lymphomas that appeared in Lck-Tert mice were disseminated, as indicated by the fact that they affected both lymphoid and nonlymphoid tissues, while none of the age-matched wild-type mice with lymphoma showed nonlymphoid tissues affected with lymphoma. This dramatic difference between Lck-Tert and wild-type mice indicates a novel role of telomerase in conferring a more-invasive phenotype on T-cell lymphoma, which is also independent of the role of telomerase in telomere length maintenance. Therefore, a putative telomerase inhibitor could impair not only the growth of tumors but also their invasive dissemination. These results are in agreement with the recent finding that the alternative mechanism for telomere maintenance is not as efficient as telomerase activity in sustaining tumor growth and dissemination, despite the fact that both mechanisms are able to maintain telomere length (11).

Tert constitutive expression could interfere with proper telomere capping and/or with correct DNA repair of lesions in the genome, especially in situations where Tert is vastly overexpressed. In particular, telomerase has been reported to change its expression and subnuclear localization in response to various types of DNA damage (8, 31). In addition, Tert has been shown to bind directly to telomeres (26), thus opening the possibility that deregulated Tert expression could affect telomere capping. In turn, uncapped telomeres interfere with proper repair of DSB in the genome and lead to increased sensitivity to IR (18, 22, 32). However, the fact that Lck-Tert thymocytes do not show increased end-to-end fusions involving telomeric sequences indicates that telomere capping is normal in these cells. Interestingly, we found that Tert overexpression in Lck-Tert mice results in greater chromosomal damage following IR. The increased chromosomal instability associated with Tert overexpression may be the consequence of a direct effect of Tert on DNA damage repair. Alternatively, Tert may increase the survival of cells harboring chromosomal damage, in agreement with a role of Tert in survival (28). In this regard, a higher percentage of metaphases showed chromosomal aberrations in Lck-Tert thymocytes than in wild-type controls. In the absence of irradiation, however, no significant differences in proliferation and survival were found between wild-type and Lck-Tert primary thymocytes (data not shown). In any case, the increased chromosomal instability of Lck-Tert thymocytes may explain, at least in part, the fact that Tert overexpression has a profound effect on T-cell lymphoma progression and especially on lymphoma dissemination in both lymphoid and nonlymphoid tissues. Future characterization of this new mouse model is warranted and will contribute to our understanding of the impact of Tert expression in the context of the organism.

ACKNOWLEDGMENTS

We are indebted to L. Criado for transgenesis and to R. Serrano, D. Esteban, J. Freire, and E. Santos for mouse care and genotyping. We thank J. F. Garcia and M. V. Fernandez for advice on the clonality assays.

A.C. is a predoctoral fellow of the Regional Government of Madrid (CAM). The M.A.B. laboratory is funded by the Swiss Bridge Cancer Research Award 2000, the Josef Steiner Cancer Award 2003, grants GEN20014856C1308 and SAF20011869 from the Ministry of Science and Technology of Spain, grant 08.1/0054/01 from the CAM, EU grants FIGHCT199900009, FIGHCT199900002, QLG1199901341, and FIS5200200078, and the Spanish National Cancer Centre (CNIO).

REFERENCES

1. **Artandi, S. E., S. Alson, M. K. Tietze, N. E. Sharpless, S. Ye, R. A. Greenberg, D. H. Castrillon, J. W. Horner, S. R. Weiler, R. D. Carrasco, and R. A. DePinho.** 2002. Constitutive telomerase expression promotes mammary carcinomas in aging mice. Proc. Natl. Acad. Sci. USA **99:**8191–8196.
2. **Blackburn, E. H.** 2001. Switching and signaling at the telomere. Cell **106:** 661–673.
3. **Blasco, M. A., M. Rizen, C. W. Greider, and D. Hanahan.** 1996. Differential regulation of telomerase activity and telomerase RNA during multi-stage tumorigenesis. Nat. Genet. **12:**200–204.
4. **Blasco, M. A., and W. C. Hahn.** 2003. Evolving views of telomerase and cancer. Trends Cell Biol. **13:**289–294.
5. **Blasco, M. A.** 2002. Telomerase beyond telomeres. Nat. Cancer Rev. **2:**627–632.
6. **Blasco, M. A.** 2003. Telomeres and cancer: a tale with many endings. Curr. Opin. Genet. Dev. **13:**70–76.
7. **Blasco, M. A.,H.-W. Lee, P. Hande, E. Samper, P. Lansdorp, R. DePinho, and C. W. Greider.** 1997. Telomere shortening and tumor formation by mouse cells lacking telomerase RNA. Cell **91:**25–34.
8. **Bouffler, S. D., M. A. Blasco, R. Cox, and P. J. Smith.** 2001. Telomeric sequences, radiation sensitivity and genomic instability. Int. J. Radiat. Biol. **77:**995–1005.
9. **Broccoli, D., L. A. Godley, L. A. Donehower, H. E. Varmus, and T. de Lange.** 1996. Telomerase activation in mouse mammary tumors: lack of detectable telomere shortening and evidence for regulation of telomerase RNA with cell proliferation. Mol. Cell. Biol. **16:**3765–3772.
10. **Chaffin, K. E., C. R. Beals, T. M. Wilkie, K. A. Forbush, M. I. Simon, and R. M. Perlmutter.** 1990. Dissection of thymocyte signalling pathways by in vivo expression of pertussis toxin ADP-ribosyltransferase. EMBO J. **9:**3821–3829.
11. **Chang, S., C. M. Khoo, M. L. Naylor, R. S. Maser, and R. A. DePinho.** 2003. Telomere-based crisis: functional differences between telomerase activation and ALT in tumor progression. Genes Dev. **17:**88–100. (Erratum, **17:**541.)
12. **Espejel, S., S. Franco, S. Rodríguez-Perales, S. D. Bouffler, J. C. Cigudosa, and M. A. Blasco.** 2002. Mammalian Ku86 mediates chromosomal fusions and apoptosis caused by critically short telomeres. EMBO J. **21:**2207–2219.
13. **Gartner, F., F. W. Alt, R. Monroe, M. Chu, B. P. Sleckman, L. Davidson, and W. Swat.** 1999. Immature thymocytes employ distinct signaling pathways for allelic exclusion versus differentiation and expansion. Immunity **10:**537–546.
14. **González-Suárez, E., J. M. Flores, and M. A. Blasco.** 2002. Cooperation between p53 mutation and high telomerase transgenic expression in spontaneous cancer development. Mol. Cell. Biol. **22:**7291–7301.
15. **González-Suárez, E., E. Samper, J. M. Flores, and M. A. Blasco.** 2000. Telomerase-deficient mice with short telomeres are resistant to skin tumorigenesis. Nat. Genet. **26:**114–117.
16. **González-Suarez, E., E. Samper, A. Ramírez, J. M. Flores, J. Martín-Caballero, J. L. Jorcano, and M. A. Blasco.** 2001. Increased epidermal tumors and increased skin wound healing in transgenic mice overexpressing the catalytic subunit of telomerase, mTERT, in basal keratinocytes. EMBO J. **20:**2619–2630.
17. **Goytisolo, F. A., and M. A. Blasco.** 2002. Many ways to telomere dysfunction: in vivo studies using mouse models. Oncogene **21:**584–591.
18. **Goytisolo, F. A., E. Samper, J. Martin-Caballero, P. Finnon, E. Herrera, J. M. Flores, S. D. Bouffler, and M. A. Blasco.** 2000. Short telomeres result in organismal hypersensitivity to ionizing radiation in mammals. J. Exp. Med. **192:**1625–1636.
19. **Hemann, M. T., M. A. Strong, L. Y. Hao, and C. W. Greider.** 2001. The shortest telomere, not average telomere length, is critical for cell viability and chromosome stability. Cell **107:**67–77.
20. **Izquierdo, M., A. Grandien, L. M. Criado, S. Robles, E. Leonardo, J. P. Albar, G. G. de Buitrago, and A. C. Martinez.** 1998. Blocked negative selection of developing T cells in mice expressing the baculovirus p35 caspase inhibitor. EMBO J. **18:**156–166.
21. **Kawamoto, H., T. Ikawa, K. Ohmura, S. Fujimoto, and Y. Katsura.** 2000. T cell progenitors emerge earlier than B cell progenitors in the murine fetal liver. Immunity **12:**441–450.
22. **Latre, L., L. Tusell, M. Martín, R. Miró, J. Egozcue, M. A. Blasco, and A. Genescá.** 2003. Shortened telomeres join DNA breaks interfering with their correct repair. Exp. Cell Res. **287:**282–288.
23. **Martin-Rivera, L., E. Herrera, J. P. Albar, and M. A. Blasco.** 1998. Expression of mouse telomerase catalytic subunit in embryos and adult tissues. Proc. Natl. Acad. Sci. USA **95:**10471–10476.
24. **Morse, H. C., III, M. R. Anver, T. N. Fredrickson, D. C. Haines, A. W. Harris, N. L. Harris, E. S. Jaffe, S. C. Kogan, I. C. MacLennan, P. K. Pattengale, and J. M. Ward, the Hematopathology Subcommittee of the Mouse Models of Human Cancers Consortium.** 2002. Bethesda proposals for classification of lymphoid neoplasms in mice. Blood **100:**246–258.
25. **Samper, E., J. M. Flores, and M. A. Blasco.** 2001. Restoration of telomerase activity rescues chromosomal instability and premature aging in Terc$^{-/-}$ mice with short telomeres. EMBO Rep. **2:**800–807.
26. **Sharma, G. G., A. Gupta, H. Wang, H. Scherthan, S. Dhar, V. Gandhi, G. Iliakis, J. W. Shay, C. S. Young, and T. K. Pandita.** 2003. hTERT associates with human telomeres and enhances genomic stability and DNA repair. Oncogene **22:**131–146.
27. **Shay, J. W., and W. E. Wright.** 2002. Telomerase: a target for cancer therapeutics. Cancer Cell **2:**257–265.
28. **Smith, L. L., H. A. Coller, and J. M. Roberts.** 2003. Telomerase modulates expression of growth-controlling genes and enhances cell proliferation. Nat. Cell Biol. **5:**474–479.
29. **Stewart, S. A., W. C. Hahn, B. F. O'Connor, E. N. Banner, A. S. Lundberg, P. Modha, H. Mizuno, M. W. Brooks, M. Fleming, D. B. Zimonjic, N. C. Popescu, and R. A. Weinberg.** 2002. Telomerase contributes to tumorigenesis by a telomere length-independent mechanism. Proc. Natl. Acad. Sci. USA **99:**12606–12611.
30. **Wildin, R. S., A. M. Garvin, S. Pawar, D. B. Lewis, K. M. Abraham, K. A. Forbush, S. F. Ziegler, J. M. Allen, and R. M. Perlmutter.** 1991. Developmental regulation of lck gene expression in T lymphocytes. J. Exp. Med. **173:**383–393.
31. **Wong, J. M., L. Kusdra, and K. Collins.** 2002. Subnuclear shuttling of human telomerase induced by transformation and DNA damage. Nat. Cell Biol. **4:**731–736.
32. **Wong, K. K., S. Chang, S. R. Weiler, S. Ganesan, J. Chaudhuri, C. Zhu, S. E. Artandi, K. L. Rudolph, G. J. Gottlieb, L. Chin, F. W. Alt, and R. A. DePinho.** 2000. Telomere dysfunction impairs DNA repair and enhances sensitivity to ionizing radiation. Nat. Genet. **26:**85–88.